DISSERTATIONES MATHEMATICAE UNIVERSITATIS TARTUENSIS
15

DISSERTATIONES MATHEMATICAE UNIVERSITATIS TARTUENSIS
15

JULIA POLIKARPUS

Optimization of elastic plastic circular plates

This study was carried out at the Tartu Observatory, Estonia.

The Dissertation was admitted on March 25, 2011, in partial fulfilment of the requirements for the degree of Doctor of Philosophy in physics (astrophysics), and allowed for defence by the Council of the Institute of Physics, University of Tartu.

Supervisors: Dr. Enn Saar,
Tartu Observatory,
Estonia

Dr. Peeter Tenjes,
Institute of Physics, University of Tartu,
Estonia

Opponents: Prof. Emeritus Mauri Valtonen,
Department of Physics and Astronomy, University of Turku,
Turku, Finland

Dr. Tõnu Viik
Tartu Observatory,
Estonia

Defence: June 3, 2011, University of Tartu, Estonia

ISSN 1406-0302
ISBN 978-9949-19-626-5 (trükis)
ISBN 978-9949-19-627-2 (PDF)

Tartu Ülikooli Kirjastus
www.tyk.ee
Tellimus nr. 200

CONTENTS

List of original publications **7**

Introduction **9**

1 Basic equations and concepts **13**
1.1 Equations of equilibrium 13
1.2 Hooke's law 15
1.3 Yield criteria 17
1.4 Associated flow rule 18

2 Bending of elastic plastic circular plates **21**
2.1 Preliminaries and basic hypotheses 21
2.2 Integration of governing equations in elastic regions 23
2.3 Elastic stage of deformation 24
2.4 Optimization of elastic circular plate 25
2.5 Solution of governing equations in plastic region in the case of diamond yield condition 25
2.6 Elastic plastic solution in the case of diamond condition 29
2.7 Elastic plastic bending of an annular plate 30
2.7.1 Elastic stage of deformation 39
2.7.2 Elastic plastic stage of deformation 40
2.7.3 Numerical results 42

3 Elastic plastic bending of stepped annular plates **48**
3.1 Problem formulation and basic hypothesis 48
3.2 Basic equations and concepts 49
3.3 General solutions in elastic and plastic regions 51
3.4 The pure elastic stage of deformation (stage I) 52
3.5 Elastic plastic stage with the hinge circle (stage II) 54
3.6 The elastic plastic stage with a plastic region of finite length (stage III) 55
3.7 Several plastic regions 55
3.8 Numerical results 56
3.9 Concluding remarks 60

4 Optimization of elastic circular plates with additional supports **61**
4.1 Formulation of the problem 61
4.2 Boundary conditions 62
4.3 Necessary optimality conditions 63

4.4 Solution of governing equations 66
4.5 Solution of the adjoint system 68
4.6 Discussion of results 71

5 Anisotropic plate **75**
5.1 Formulation of the problem 75
5.2 Equations of equilibrium and strain components 75
5.3 Constitutive equations 77
5.4 Solution of governing equations 78
5.5 Bending of a one-stepped plate 81
5.6 Optimal design of a stepped plate 83
5.7 Numerical results and discussion 84
5.8 Conclusions 85

Acknowledgements **87**

References **88**

Summary in Estonian **92**

Attached original publications **97**

Curriculum vitae **171**

Elulookirjeldus **175**

LIST OF ORIGINAL PUBLICATIONS

This thesis is based on the following publications:

I **Tempel, E.**, Einasto, J., Einasto, M., Saar, E., & Tago, E. 2009, *Anatomy of luminosity functions: the 2dFGRS example*, Astronomy & Astrophysics, 495, 37

II Tago, E., Saar, E., **Tempel, E.**, Einasto, J., Einasto, M., Nurmi, P., & Heinämäki, P. 2010, *Groups of galaxies in the SDSS data release 7. Flux- and volume-limited samples*, Astronomy & Astrophysics, 514, A102

III **Tempel, E.**, Tamm, A., & Tenjes, P. 2010, *Dust-corrected surface photometry of M 31 from Spitzer far-infrared observations*, Astronomy & Astrophysics, 509, A91

IV **Tempel, E.**, Tuvikene, T., Tamm, A., & Tenjes, P. 2011, *SDSS surface photometry of M 31 with absorption corrections*, Astronomy & Astrophysics, 526, A155

V **Tempel, E.**, Saar, E., Liivamägi, L. J., Tamm, A., Einasto, M., Einasto, J., & Müller, V. 2011, *Galaxy morphology, luminosity, and environment in the SDSS DR7*, Astronomy & Astrophysics, 529, A53

Other related publications of the dissertant:

VI **Tempel, E.** & Tenjes, P. 2006, *Line-of-sight velocity dispersions and a mass-distribution model of the Sa galaxy NGC 4594*, Monthly Notices of the Royal Astronomical Society, 371, 1269

VII Tago, E., Einasto, J., Saar, E., **Tempel, E.**, Einasto, M., Vennik, J., & Müller, V. 2008, *Groups of galaxies in the SDSS Data Release 5. A group-finder and a catalogue*, Astronomy & Astrophysics, 479, 927

VIII Einasto, M., Tago, E., Saar, E., Nurmi, P., Enkvist, I., Einasto, P., Heinämäki, P., Liivamägi, L. J., **Tempel, E.**, Einasto, J., Martínez, V. J., Vennik, J., & Pihajoki, P. 2010, *The Sloan Great Wall. Rich clusters*, Astronomy & Astrophysics, 522, A92

Author's contribution to the publications

Author's research has given an essential contribution to all these publications. Here the author's contribution to the original publications is indicated. The Roman numerals correspond to those in the list of publications.

Publication I. The author performed the calculations of the luminosity functions. He designed the structure of the paper, prepared all the figures, and did most of the writing. He is responsible for the interpretation of the results, presented in this paper.

Publications II and VII. The author contributed to the preparation of the initial SDSS galaxy catalogue and is responsible for the calculation of the observed and total luminosities of galaxy groups. He contributed significantly to the development of the method to restore the total luminosities of galaxy groups.

Publications III and IV. The author contributed significantly to the development of the algorithm for the 3-dimensional galaxy modelling and to the dust-extinction calculations. He is entirely responsible for writing and developing the software package for galaxy modelling and did all the debugging and testing. For the SDSS data for M 31, he reduced most of the observational data. He did all the model calculations, and prepared most of the figures. He designed the structure of the papers and did most of the writing.

Publication V. The author is responsible for the morphological classification, derived in this paper. He carried out all the luminosity function calculations. He is responsible for most of the interpretations, based on the calculated luminosity functions. He designed the structure of the paper, prepared all the figures, and did most of the writing.

Publication VI. The author derived the formulae to calculate the observed rotational velocities and dispersions of the stellar components of a galaxy. He wrote the necessary software package for model calculations. He is responsible for the kinematical calculations, presented in this paper. He prepared all the figures and did about half of the writing.

Publication VIII. The author is responsible for data preparation that was essential for this study. Most, but not all, data preparation was done during the work on the Papers II and VII. He is responsible for many ideas, which make this paper more clear and readable.

INTRODUCTION

The reduction of the structural compliance of thin walled beams, plates and shells is often the primary concern in the engineering mechanics. The need for reduction of the compliance and the increase of the structural stiffness is related to the use of light-weight structures which are less material consuming than the traditional structures.

It is wellknown that the structural material is used in more efficient manner and the ratio of the strength to weight is larger if inelastic deformations are taken into account when designing the structure. Although the early results of the behaviour of elastic plastic circular and annular plates have obtained a long ago by Naghdi [28], Hodge (1960), Tekinalp (1956) the most of the attention is paid to plates of constant thickness only. Comprehensive reviews of these investigations can be found in the books by Chakrabarty [7], Cohn [8], Kaliszky [13], Save, Massonnet, Saxce [34], Yu, Zhang [44]. Hodge introduced an essential simplification of inelastic problems in the case of a Tresca material making use of the yield surface consisting of two hexagons on the planes of moments and membrane forces, respectively. It was used by many investigators for getting approximate solutions. Among others, Sherbourne, Srivastava [36] found an analytical solution to the elastic plastic bending problem in the range of large deflections.

The exact analysis of elastic plastic plates is quite complicated. This involves the need for physically reasonable simplifications. An effective simplification is introduced by Haythornthwaite (1955) and Tekinalp (1956, 1957). Haythornthwaite suggested to assume that any plate element is either entirely elastic or entirely plastic. This assumption is fulfilled in the case of a sandwich plate consisting of two carrying layers and of a core material between the rims. Haythornthwaite (1955) investigated the elastic plastic bending of an annular plate loaded by the central absolutely rigid boss. The plate is clamped to the boss at the inner edge and simply supported at the outer edge. An exact theoretical solution is derived for a plate made of a Tresca material.

Tekinalp (1956) studied the circular plate simply supported at the edge and subjected to the uniformly distributed transverse pressure. The solution for a plate clamped at the outer edge was obtained a little later Tekinalp [38]. The solutions in both cases consist of the initial elastic stage and several subsequent elastic plastic stages of deformation.

The complete elastic plastic analysis of centrally clamped annular plates carrying uniformly distributed transverse loading was undertaken by French [10] within the frame works of the pure bending theory of thin plates. Exact stress profiles lying partly inside and partly on the yield hexagon are developed for the elastic and elastic

plastic stages of the deformation. It is assumed by French [10] that the plate is a sandwich construction and that the material of carrying layers obeys the Tresca yield condition. The elastic plastic bending of circular and annular plates made of a Tresca material was also studied by Hodge (1960, 1968).

Elastic plastic deformations of axisymmetric plates made of a von Mises material are investigated by Eason [9], Sokolovski (), Lackman (1964), Popov et al (1967), Turvey (1979), Turvey and Lim (1984), Turvey and Salehi (1991), Ohashi and Murakami (1964).

The classical concept of an elastic plastic body admits the exact definition of yielding and of the yield-point load. It is shown earlier by Tekinalp (1956), Hodge (1960) and others that in the case of the Tresca material and a plate subjected to the uniformly distributed transverse pressure of intensity p the onset of yielding corresponds to the values of the pressure $p = \dfrac{16M_0}{R^2(3+\nu)}$ and $p = \dfrac{8M_0}{R^2}$ for simply supported and clamped plates, respectively. Here ν is the Poisson ratio, R and M_0 stand for the radius of the plate and the yield moment of the material, respectively. The concept of gradual yielding introduced by Richard and Abbott (1975) for one-dimensional structures was extended to circular and annular plates by Upadastra, Peddieson, Buchanan (2006) and Khalili, Peddieson (2013).

Elastic plastic bending of axisymmetric plates in the range of large deflections was investigated by Ohashi, Murakami, Endo (1967), Sherbourne and Srivastava (1971), also Gorji and Akileh (1990), Turvey (1978). Stress and strain distributions in rotating disks made of a Tresca material are determined by Güven (1992) and Gamer (1985). In the cited papers solid and sandwich plates and rotating disks are investigated assuming that the material is an ideal elastic plastic material without strain hardening. Plates made of a hardening material were studied by Boyce (1959), Hwang (1960), Tanaka (1972). Wen (1998), Kirs, Kenk (1990) considered work-hardening circular plates subjected to dynamic loading under different circumstancies.

The use of the classical bending theory based on Kirchhoff hypotheses is justified in the case of thin plates and homogeneous materials. In more complicated cases the shear stresses must be taken into account as shown by Oblak (1986), Nagai and Ito (1991). Sawczuk and Puszck (1963) developed similar concept for ideal plastic plates.

Reddy and Wang (1997) investigated relationships between the classical pure bending theory and the shear deformation theory applied to the bending of circular and annular plate. The full discription of the shear deformation theory of plates and shells can be found in the book by Wang, Reddy, Lee (2009).

One of the ways of increasing the stiffness of beams, plates and shells is to furnish these structural elements with additional supports. Evidently, it is reasonable to settle

these supports at the optimal positions.

The problem of minimization of the compliance of elastic beams and the determination of the optimal location of the additional support was first formulated by Mroz and Rozvany [27]. In paper Mroz and Rozvany [27] designs of minimumcompliance of beams are established in the case of quasistatic loading. Later Szelag and Mroz [37], Akesson and Olhoff [1] treated the problems of maximal eigenfrequency for given stiffness with respect to the location of the additional support. Bojczuk and Mroz [4] developed a new method for simultaneous optimization of topology, configuration and cross-sectional dimensions of elastic beams and beam structures extending earlier results by Garstecki and Mroz [11], Mroz and Lekszycki [27], also by Lepik [26]. In the subsequent papers by Bojczuk and Mroz [5] this concept was applied for optimal design of active supports with force actuators. Olhoff and Akesson [29] treated the stability of columns and Wang et al [42] studied the buckling of axisymmetric plates.

A lot of attention has been paid in the literature to the optimization of internal supports to beam, plate and shell structures in the case of inelastic materials. Probably the first paper in this area is due to Prager and Rozvany [31]. Systematic reviews of results obtained in earlier papers are presented by Rozvany [33], also by Lellep and Lepik [18]. Optimal designs of circular cylindrical shells with additional supports are established by Lellep [14, 17] in the case of dynamic loading and an ideal plastic material. The behaviour of geometrically non-linear cylindrical shells with internal supports is studied in [16, 15, 17, 19].

Optimal designs of axisymmetric plates and shells of various shape made of elastic and inelastic materials are established in [22, 23, 24, 25]. Inelastic spherical and conical shells are studied in [23, 24, 25] whereas a stress strain analysis of an annular plate made of an elastic plastic material is presented in [21].

A design sensitivity analysis for the deflection of beam or plate structures was undertaken by Wang [43] in the case of simple supports located at given mesh nodes. Stiffened sector plates are studied in [39].

In the present work an analytical method of determination of positions of rigid ring supports for circular plates is developed. The analysis is confied to the axisymmetric response of elastic plates to subjected loads.

Plates and shells are widely used in various fields of technology and engineering. The behaviour of plates and shells in the range of elastic deformations has been studied by many authors (see [32]; [41]; [40]).

The practical need for light weight structures has increased the importance of investigations of composite materials, also sandwich plates and shells and of these manufractured from composites. The foundations of the analysis and design of sandwich structures was developed by Allen [2] and Plantema [30]. The stability problem

of a three-layered plate with a soft core was solved by Pawlus []. The critical loads are obtained analytically and numerically. Elastic circular sandwich plates subjected to the ring load have studied by Magnucki, Jasion et al (2014). The comparison of the analytical, numerical and experimental results reveals small discrepancies between theoretical predictions and experimental data. These are probably due to the approximate determination of the mechanical properties of the core material. The influence of shear forces on the bending of circular plates was studied by Reddy, Wang (1997).

There exists a large number of books dedicated to the foundations of composite materials. It is worthwhile to mention among others the books by Herakovich (1998), Jones (1999).

In the present work the elastic plastic bending of annular plates of piecewise constant thickness is studied. It is assumed that the material of the plate clamped at the inner edge is an ideal plastic one obeying the square yield condition.

CHAPTER 1
BASIC EQUATIONS AND CONCEPTS

In this chapter the governing equations for thin plates are prsented. This system of equations consists of the equations of equilibrium and of the physical relations for elastic and plastic regions for the thin-walled circular and annular plates will be presented. For the sake of simplicity a thin-walled plate with constant thickness is considered.

1.1 Equations of equilibrium

We consider axisymmetric deformations of a circular plate subjected to the axisymmetric transverse loading of intensity $P = P(r)$. Here r is the current radius e. g. the distance from the center of the plate. As we are studying the axisymmetric response of the plate all points lying at the circle with radius r have common displacements $W(r)$ in the transverse direction as well as common deformations and curvatures κ_1, κ_2 in the radial and circumferential directions, respectively. Note that the radial displacement will be neglected in the present study since the classical equations of the bending theory of thin plates will be used.

In the present study we shall employ the linear theory of thin plates (see Reddy [32], Vinson [41]). According to this approach one can treat the equilibrium of internal and external forces and couples on the basis of an undeformed element of the plate. Let M_1, M_2 be the generalized couples called bending moments in the radial and circumferential directions, respectively. Bending moments M_1, M_2 are the only generalized stress components contributing to the internal energy. Note that the membrane forces are assumed to be small so that one can neglect the membrane action of internal forces. Although the shear force Q may be finite it does not contribute to the internal energy in the classical plate theory. The reason is that the corresponding strain component vanishes.

In the frameworks of the classical plate theory where axial symmetry is retained the couples M_1, M_2 with forces Q and P form a system of forces and moments which keep the element of the plate in equilibrium. The equilibrium conditions of the plate

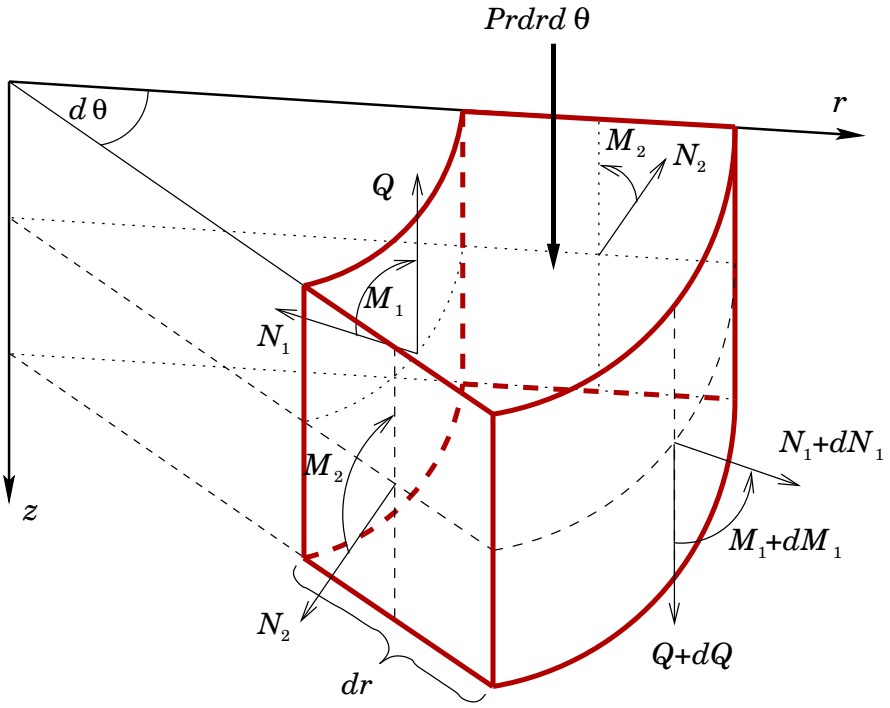

Figure 1.1: An element of the circular plate.

element presented in Fig. 1.1 can be written as

$$\begin{aligned} &\frac{d}{dr}(rN_1) - N_2 = 0, \\ &\frac{d}{dr}(rM_1) - M_2 - rQ = 0, \\ &\frac{d}{dr}(rQ) + P(r)r = 0. \end{aligned} \tag{1.1}$$

Note that in the following the influence of membrane forces N_1, N_2 will be neglected.

1.2 Hooke's law

If the material of the plate is an ideal elastic material the Hooke's law holds good. In the case of an isotropic elastic material The Hooke's law reads

$$\begin{aligned}
\varepsilon_1 &= \frac{1}{E}[\sigma_1 - \nu(\sigma_2 + \sigma_3)]; \qquad \gamma_{12} = \frac{\tau_{12}}{G};\\
\varepsilon_2 &= \frac{1}{E}[\sigma_2 - \nu(\sigma_1 + \sigma_3)]; \qquad \gamma_{13} = \frac{\tau_{13}}{G};\\
\varepsilon_3 &= \frac{1}{E}[\sigma_3 - \nu(\sigma_1 + \sigma_2)]; \qquad \gamma_{23} = \frac{\tau_{23}}{G}.
\end{aligned} \tag{1.2}$$

Here ε_j, γ_j $(j = 1, 2, 3)$ stand for strain components whereas σ_j, τ_j $(j = 1, 2, 3)$ are stress components; E is the Young modulus, ν is Poisson ratio and $G = \dfrac{E}{2(1+\nu)}$. In the case of plane stress state when $\varepsilon_3 = 0$, $\tau_{23} = \sigma_3 = 0$ one has

$$\begin{aligned}
\varepsilon_1 &= \frac{1}{E}(\sigma_1 - \nu\sigma_2),\\
\varepsilon_2 &= \frac{1}{E}(\sigma_2 - \nu\sigma_1),\\
\gamma_{12} &= \frac{\tau_{12}}{G}
\end{aligned} \tag{1.3}$$

or in the inverted form as

$$\begin{aligned}
\sigma_1 &= \frac{E}{1-\nu^2}(\varepsilon_1 + \nu\varepsilon_2),\\
\sigma_2 &= \frac{E}{1-\nu^2}(\varepsilon_2 + \nu\varepsilon_1),\\
\tau_{12} &= G\gamma_{12}.
\end{aligned} \tag{1.4}$$

The strain components can be expressed via displacements u, v, w in the direction of coordinate axes, respectively. Making use of polar coordinates (now u is directed in the radial direction and v in the circumferential direction) one has

$$\begin{aligned}
\varepsilon_1 &= \frac{\partial u}{dr},\\
\varepsilon_2 &= \frac{u}{r} + \frac{1}{r}\frac{\partial v}{\partial \Theta},\\
\gamma_{12} &= \frac{\partial v}{\partial r} - \frac{v}{r} + \frac{1}{r}\frac{\partial u}{\partial \Theta}.
\end{aligned} \tag{1.5}$$

In the case axisymmetric loading it is expected that the stress-strain state is also axisymmetric, provided the boundary conditions at the edges of the plate are axisymmetric. Now the displacements do not depend on the polar angle Θ and one has

$$\begin{aligned} \varepsilon_1 &= \frac{du}{dr}, \\ \varepsilon_2 &= \frac{u}{r}, \\ \gamma_{12} &= \frac{dv}{dr} - \frac{v}{r}. \end{aligned} \tag{1.6}$$

According to Kirchhoff hypotheses one has (see Reddy [32], Vinson [41])

$$\begin{aligned} \varepsilon_1 &= z\varkappa_1, \\ \varepsilon_2 &= z\varkappa_2 \end{aligned} \tag{1.7}$$

where z is the distance between a current point and the middle surface of the plate. Principal curvatures $\varkappa_1$, $\varkappa_2$ can be expressed as

$$\begin{aligned} \varkappa_1 &= -\frac{d^2W}{dr^2}, \\ \varkappa_2 &= -\frac{1}{r}\frac{dW}{dr} \end{aligned} \tag{1.8}$$

where W is the transverse deflection or displacement in the z-axis of points lying on the middle surface.

Let us introduce the generalized stresses (bending moments)

$$\begin{aligned} M_1 &= \int_{-\frac{h}{2}}^{\frac{h}{2}} \sigma_1 z dz, \\ M_2 &= \int_{-\frac{h}{2}}^{\frac{h}{2}} \sigma_2 z dz, \\ M_{12} &= \int_{-\frac{h}{2}}^{\frac{h}{2}} \tau_{12} z dz \end{aligned} \tag{1.9}$$

and the shear force

$$Q = \int_{-\frac{h}{2}}^{\frac{h}{2}} \tau_{13} dz. \tag{1.10}$$

Substituting equations (1.4) with (1.7), (1.8) in (1.9) after integration one has

$$\begin{aligned} M_1 &= D(\varkappa_1 + \nu\varkappa_2), \\ M_2 &= D(\varkappa_2 + \nu\varkappa_1) \end{aligned} \tag{1.11}$$

where

$$D = \frac{Eh^3}{12(1-\nu^2)} \tag{1.12}$$

in the case of a solid plate and

$$D = \frac{EhH^2}{2(1-\nu^2)} \tag{1.13}$$

in the case of a sandwich plate. In (1.13) H stands for the total thickness and h is the thickness of carrying layers.

The stress strain state is determined according to equations (1.1). Substituting equations (1.11), (1.8) in formula (1.1) leads to a fourth order equation with respect to the deflection W known from the theory of elastic plates (see Reddy [32], Vinson [41]; Ventsel, Krauthammer [40])

$$\frac{1}{r}\frac{d}{dr}\left\{r\frac{d}{dr}\left[\frac{1}{r}\frac{d}{dr}\left(r\frac{dW}{dr}\right)\right]\right\} = \frac{P(r)}{D}. \tag{1.14}$$

The general solution of this equation can be presented in the case $P = const$ as

$$W = \frac{Pr^4}{64D} + A_1 r^2 \ln r + A_2 r^2 + A_3 \ln r + A_4 \tag{1.15}$$

where A_1 – A_4 are the integration constants.

1.3 Yield criteria

The theories of plasticity are based on experimental observations regarding the behaviour of inelastic materials. The experiments show that a rod in a simple tension test remains elastic until the stress does not exceed a limit value, called the yield stress σ_0. In this thesis it is assumed that the stress strain curve can be approximated by two straight lines shown in Fig. 1.2. Thus, according to this model a one-dimensional body (a rod under tension) remains elastic if $|\sigma| < \sigma_0$.

However, in the general case the stress state of a material element can be represented by a point in a nine-dimensional stress space with coordinates σ_{ij} $(i, j = 1, 2, 3)$. Theoretical considerations and experimental investigations show that around the origin of the stress space there exists a closed convex surface

$$\Phi_0(\sigma_{11}, \sigma_{12}, \ldots, \sigma_{33}) = 0 \tag{1.16}$$

surrounding the region where elastic deformations take place. The points lying on this surface correspond to the points of the body where plastic deformations occur.

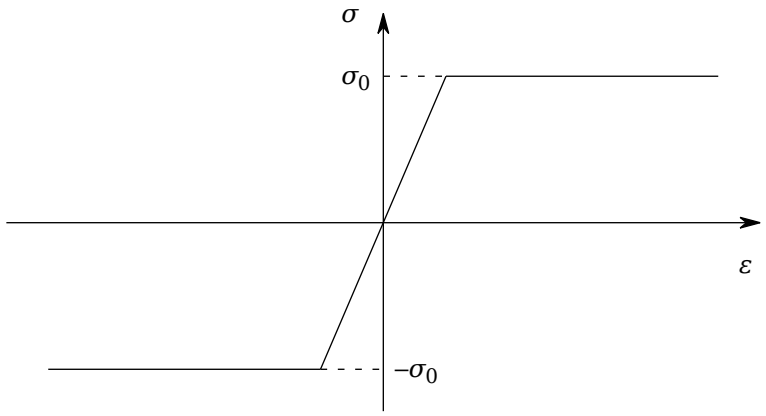

Figure 1.2: The stress-strain curve.

In the case of axisymmetric thin-walled plates the yield surface (1.16) can be expressed via bending moments as

$$\Phi(M_1, M_2, M_0) = 0 \tag{1.17}$$

where M_0 stands for the yield moment. Evidently

$$M_0 = \frac{\sigma_0 h^2}{4} \tag{1.18}$$

for solid plates and

$$M_0 = \sigma_0 h H \tag{1.19}$$

for sandwich plates.

The most often used yield conditions are the Tresca (Fig. 1.3) and Mises (Fig. 1.4) conditions.

1.4 Associated flow rule

In the general case the yield criterion $\Phi \leq 0$ holds good. In an elastic region one has $\Phi < 0$ and in a plastic region $\Phi = 0$. In the theory of plasticity it is shown that in a plastic region of a body where $\Phi = 0$ the strain rate vector $\dot{\vec{\varepsilon}}$ is directed outwards the yield surface (see Chakrabarty [7], Kaliszky [13]; Sawczuk, Sokól-Supel [35]). Thus

$$\dot{\varepsilon}_{ij} = \frac{\lambda \partial \Phi_0}{\partial \sigma_{ij}} \tag{1.20}$$

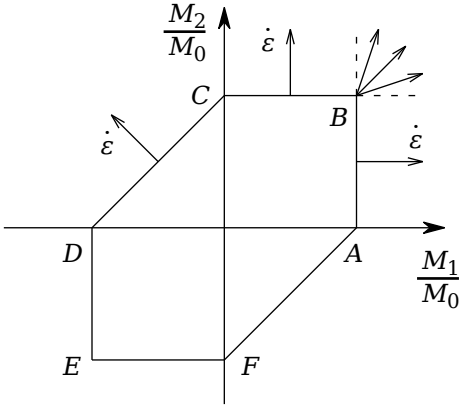

Figure 1.3: Tresca's yield hexagon.

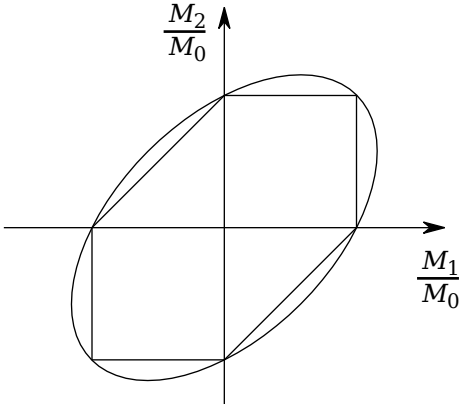

Figure 1.4: Von Mises yield ellipse.

for $i, j = 1, 2, 3$. In equation (1.20) λ stands for a non-negative scalar multiplier and the dot denotes the derivative with respect to time. Using the generalized stresses and the yield surface in the form (1.17) one has

$$\begin{aligned} \dot{\varkappa}_1 &= \frac{\lambda \partial \Phi}{\partial M_1}, \\ \dot{\varkappa}_2 &= \frac{\lambda \partial \Phi}{\partial M_2} \end{aligned} \tag{1.21}$$

where $\varkappa_1$, $\varkappa_2$ stand for the curvatures.

At the non-regular points of the yield surface the strain rate vector is formed as a linear combination with unknown coefficients of outward normals to the adjacent portions of the yield surface.

Note that in the "deformation theory" of plasticity instead of strain rate the strain components themselves are used.

Let us consider the case when the behaviour of the material in plastic stage corresponds to Tresca's yield condition (Fig. 1.3) and to associated gradientality law in a greater detail. The latter means that if the stress point is lying at an edge of Tresca's hexagon then the vector of curvatures with components (1.8) is directed towards the external normal to the edge. It will be shown that in the case of a circular plate subjected to unidirectional transverse loading the yield regime $M_2 = M_0$ takes place, where M_0 stands for the yield moment.

If the stress state of the plate corresponds to an internal point of the side BC of the yield hexagon, then according to the gradientality law $\dot{\varkappa}_1 = 0$, $\dot{\varkappa}_2 \geq 0$. Thus

$$\frac{d^2\dot{W}}{dr^2} = 0 \tag{1.22}$$

in this case. Making use of the deformation theory the general solution of the equation (1.22) can be presented as

$$W = Ar + B \tag{1.23}$$

where A and B are the constants of integration.

If the stress strain state of the plate in certain region corresponds to a non-regular point of the yield curve (for instance, the corner point B in Fig. 1.3), then the strain rate vector lies inside the angle formed by external normals to crossing sides.

At the point B of the Tresca hexagon (Fig. 1.3) $M_1 = M_2 = M_0$ and the associated yield law states that $\dot{\varkappa}_1 \geq 0$, $\dot{\varkappa}_2 \geq 0$. Thus the exact expressions of strain rates remain unknown here.

Note that if the stress strain state corresponds to an interiour point of the yield hexagon (Fig. 1.3) then the plate material remains elastic in this region and Hooke's law holds good.

CHAPTER 2
BENDING OF ELASTIC PLASTIC CIRCULAR PLATES

2.1 Preliminaries and basic hypotheses

Let us consider the quasistatic behaviour of an elastic plastic circular plate of radius R under the lateral pressure of intensity $P = P(r)$, r being the current radius. It is assumed that the plate is of sandwich-type consisting of carrying layers of thickness h and of a core material between the rims. The thickness of the layer of the core material is H. We assume that

$$h = h_j, \tag{2.1}$$

for $r \in (a_j, a_{j+1})$; $j = 0, \ldots, n$. The quantities a_j, h_j are treated as preliminary known parameters. For the sake of convenience we take $a_0 = 0$; $a_{n+1} = R$. The response of the plate to the external loading will be prescribed by the classical plate theory. The stress components contributing to the strain energy are the bending moments M_1, M_2 in the radial and hoop direction, respectively. Corresponding strain components are the curvatures $\varkappa_1$, $\varkappa_2$ which can be determined via the transverse deflection $W = W(r)$.

It is assumed that the radial bending moment M_1 as well as the shear force Q, deflection W and slope dW/dr are continuous for each $r \in (0, R)$. However, the deflection slope may have discontinuities at sections where $M_1 = M_0$ (see Chakrabarty (2006), Kachanov (), Yu Chang ()). It means that

$$\begin{aligned} &[W(a_j)] = 0, \\ &\left[\frac{dW(a_j)}{dr}\right] = 0, \\ &[M_1(a_j)] = 0 \end{aligned} \tag{2.2}$$

and

$$(|M_1(a_j)| - M_0)\left[\frac{dW(a_j)}{dr}\right] = 0. \tag{2.3}$$

The aim of this chapter is to determine the stress strain state of the plate for the initial elastic and subsequent elastic plastic stages of loading.
If the load intensity is high enough plastic deformations occur in certain regions. Now the plate is divided into elastic and plastic regions. Let us denote these regions S_e and S_p, respectively. In a plastic region the stress state corresponds to a point lying on the yield surface (or a yield curve). It is assumed that the yield condition can

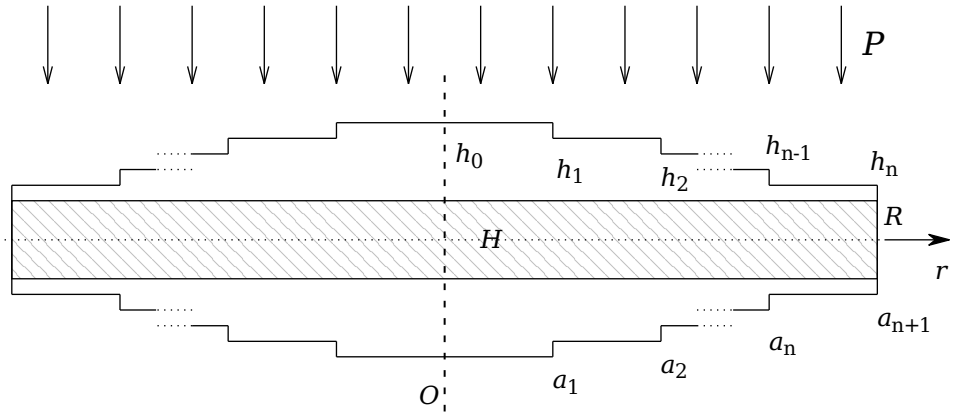

Figure 2.1: Cross-section.

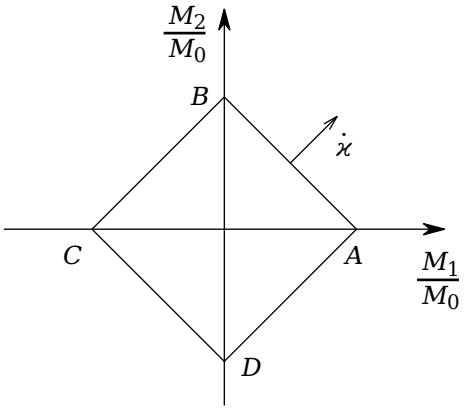

Figure 2.2: Diamond yield condition.

be presented by the diamond $ABCD$ shown in Fig. 2.2. Here M_{0j} denotes the yield moment. In the case of a sandwich plate with the rim thickness h_j

$$M_{0j} = \sigma_0 h_j H, \tag{2.4}$$

σ_0 being the yield stress of the material. Since $M_1 \geq 0$, $M_2 \geq 0$ in the most cases one can assume that in the plastic region

$$M_1 + M_2 = M_{0j} \tag{2.5}$$

for $r \in (a_j, a_{j+1})$. Note that the diamond yield condition was suggested by Jones [3] for approximate solution of dynamic problems of plastic plates.

According to the associate flow law on the side AB of the diamond one has $\dot{\varkappa}_1 = \dot{\varkappa}_2$ where dots denote the differention with time or a time-like parameter. Making use of (1.8) and the deformation-type theory of plasticity the gradientality law results in the equation

$$\frac{d^2W}{dr^2} - \frac{1}{r}\frac{dW}{dr} = 0. \tag{2.6}$$

2.2 Integration of governing equations in elastic regions

Assume that the portion of the plate for $r \in (a_j, a_{j+1})$ is in pure elastic stress-strain state. For determination of stresses, strains and displacement one has the equations (1.1)–(1.11). Substituting (1.11) with the help of (1.8) in the equilibrium equations (1.1) results in

$$\frac{1}{r}\frac{d}{dr}\left\{r\frac{d}{dr}\left[\frac{1}{r}\frac{d}{dr}\left(r\frac{dW}{dr}\right)\right]\right\} = \frac{P(r)}{D_j} \tag{2.7}$$

for $r \in (a_j, a_{j+1})$ and where

$$D_j = \frac{Eh_jH^2}{2(1-\nu^2)}. \tag{2.8}$$

This is true under the condition that this intervalt belongs to the set S_e.
One can easily recheck that the general solution of the equation (2.7) is

$$W = A_{1j}r^2\ln r + A_{2j}r^2 + A_{3j}\ln r + A_{4j} + \frac{Pr^4}{64D_j} \tag{2.9}$$

where $A_{1j} - A_{4j}$ are arbitrary constants.
Bending moments have the form

$$\begin{aligned}
M_1 &= -D_j\left\{\frac{Pr^2(3+\nu)}{16D_j} + A_{1j}[2\ln r + 3 + \nu(2\ln r + 1)]\right.\\
&\left.+2A_{2j}(1+\nu) + \frac{A_{3j}(\nu-1)}{r^2}\right\},\\
M_2 &= -D_j\left\{\frac{Pr^2(1+3\nu)}{16D_j} + A_{1j}[2\ln r + 1 + \nu(2\ln r + 3)]\right.\\
&\left.+2A_{2j}(1+\nu) + \frac{A_{3j}(1-\nu)}{r^2}\right\}.
\end{aligned} \tag{2.10}$$

2.3 Elastic stage of deformation

In the case of smaller values of the intensity of the transverse pressure the plate remains elastic. In the elastic stage the stress strain state of the plate is defined by (2.9) and (2.10).

Let us consider now a particular case of the problem posed above when $n = 1$ and the thickness distribution is

$$h = \begin{cases} h_0, & r \in [0, a] \\ h_1, & r \in [a, R]. \end{cases} \tag{2.11}$$

Let the applied loading be of constant intensity. For the concreteness sake let us assume that the plate is simply supported at the edge. Thus at the boundary of the plate

$$\begin{aligned} M_1(R) &= 0, \\ W(R) &= 0. \end{aligned} \tag{2.12}$$

Here in (2.9) and (2.10) one has to take $j = 0$, if $r \in [0, a]$ and $j = 1$, if $r \in [a, R]$.

Calculating the shear force for the elastic plate one reaches to the relation

$$Q = \frac{1}{r}\left(\frac{d}{dr}(rM_1) - M_2\right). \tag{2.13}$$

Substituting M_1, M_2 from (2.10) in (2.13) one can see that the shear force is continious all over the plate and thus constants $A_{1j} = 0$.

Evidently, $M_1(0)$ must be finite. Thus it follows from (2.9) that $A_{30} = 0$. For determination of the rest unknown constants A_{20}, A_{40}, A_{21}, A_{31}, A_{41}, one can use the boundary conditions (2.12) and the continuity requirements

$$\begin{aligned} [W(a)] &= 0, \\ [M_1(a)] &= 0, \\ \left[\frac{dW(a)}{dr}\right] &= 0. \end{aligned} \tag{2.14}$$

Here and now on square brackets denote finite jumps of corresponding variables at the given points. From the first equation in (2.12) one can express the constant

$$A_{21} = \frac{-PR^2(3+\nu)}{32D_1(1+\nu)} + \frac{A_{31}(1-\nu)}{2R^2(1+\nu)}. \tag{2.15}$$

Substituting the constant A_{21} from equation (2.15) into the second equation in (2.12) one can determine

$$A_{41} = \frac{PR^4(5+\nu)}{64D_1(1+\nu)} - \frac{A_{31}[1-\nu+2(1+\nu)\ln R]}{2(1+\nu)}. \tag{2.16}$$

Making use of the continuity of the bending moment M_1 at $r = a$ in (2.14) and equation (2.15) one can express

$$A_{20} = \frac{-PR^2(3+\nu)}{32D_0(1+\nu)} + \frac{A_{31}D_1(1-\nu)(a^2-R^2)}{2D_0(1+\nu)R^2a^2}. \tag{2.17}$$

Substituting the constants A_{20}, A_{21} and A_{41} into the first equation in (2.14) one can obtain

$$\begin{aligned} &A_{40} \\ &= \frac{P[a^4(1+\nu)(D_0-D_1)+R^4D_0(5+\nu)+2R^2a^2(3+\nu)(D_1-D_0)]}{64D_0D_1(1+\nu)} \\ &+\frac{A_{31}\{(1-\nu)[(R^2-a^2)D_1+a^2D_0]+D_0R^2[2(1+\nu)(\ln a-\ln R)-1+\nu]\}}{2D_0(1+\nu)R^2}. \end{aligned} \tag{2.18}$$

Finally, making use of equations (2.17), (2.15) and the third equation in (2.14) one can express

$$A_{31} = \frac{Pa^2R^2(D_1-D_0)[a^2(1+\nu)-R^2(3+\nu)]}{16D_1\{D_0[a^2(1-\nu)+R^2(1+\nu)]+D_1(\nu-1)(a^2-R^2)\}}. \tag{2.19}$$

2.4 Optimization of elastic circular plate

2.5 Solution of governing equations in plastic region in the case of diamond yield condition

In plastic region one has to satisfy the equations (2.5), (2.6) and the equilibrium equations (1.1). Integrating (2.6) one easily obtains

$$W = Ar^2 + B \tag{2.20}$$

A and B being arbitrary constants. For determination of stress components one can use equations (1.1) and (2.5). The second equation in system (1.1) gives after integration

$$Q = -\frac{1}{r}\int P(r)rdr + C_1. \tag{2.21}$$

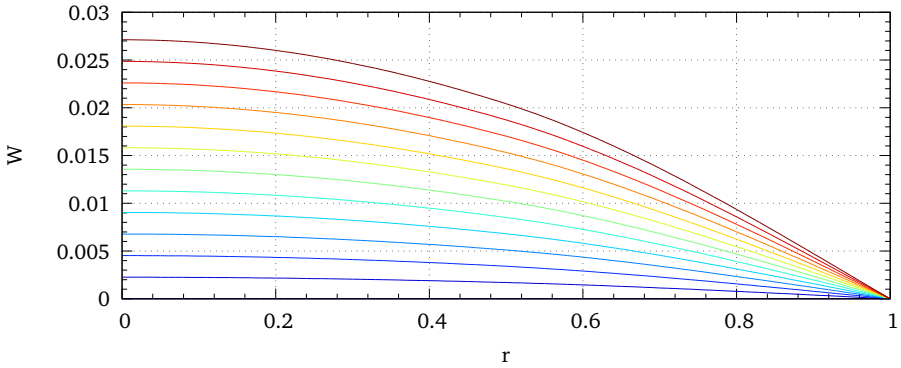

Figure 2.3: Deflection a05Rg05.

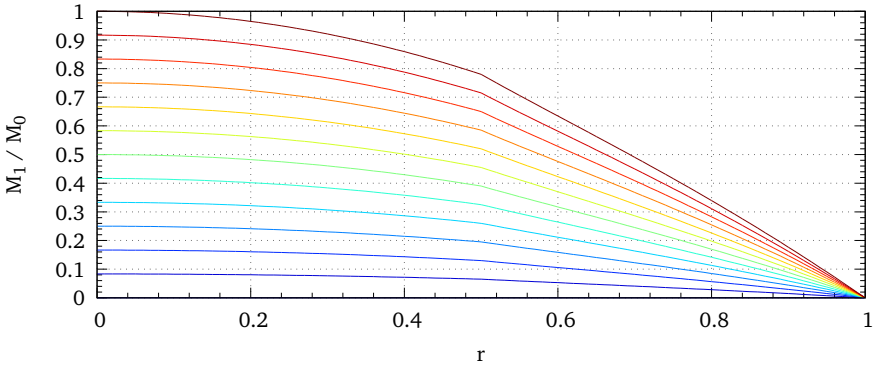

Figure 2.4: Bending moment a05Rg05.

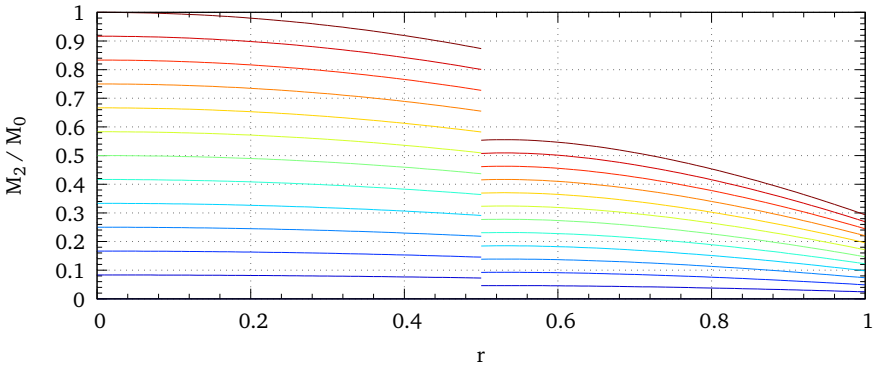

Figure 2.5: Circumferential moment a05Rg05.

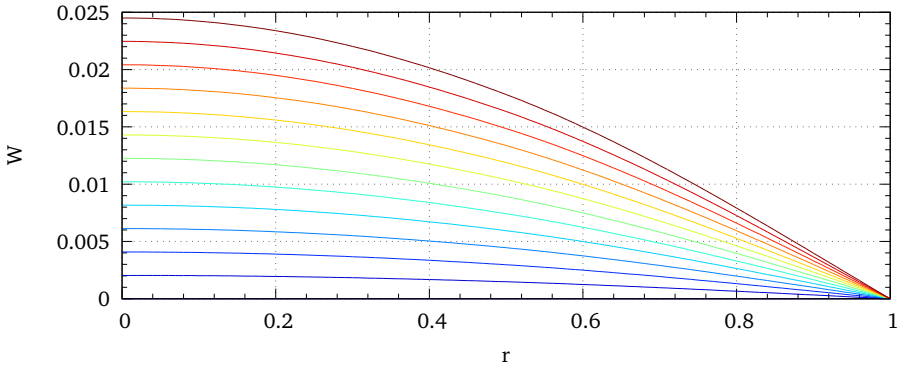

Figure 2.6: Deflection a05Rg07.

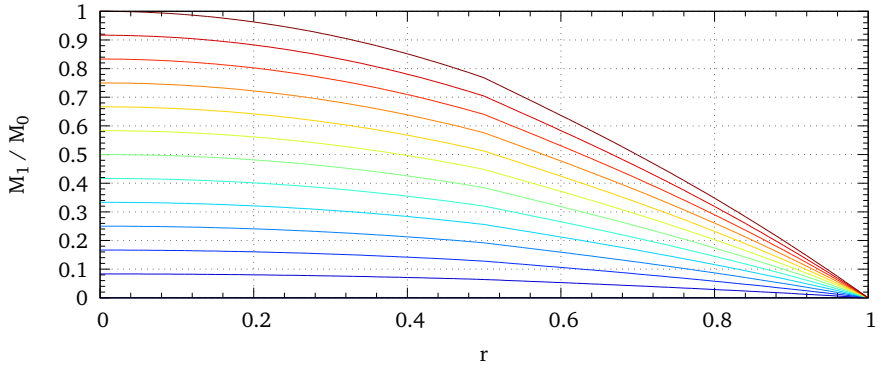

Figure 2.7: Bending moment a05Rg07.

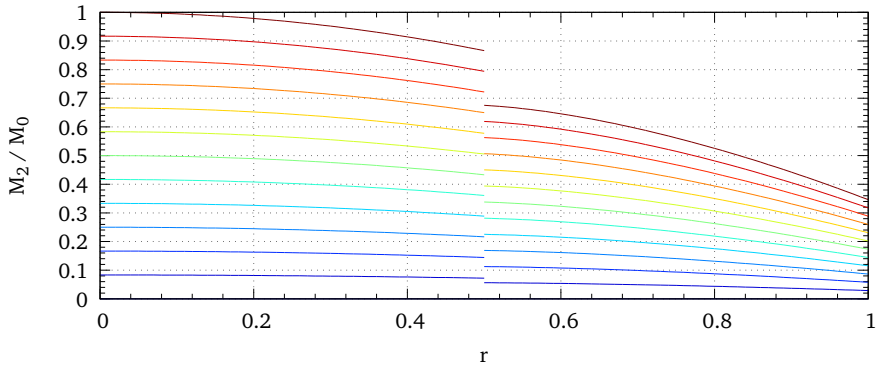

Figure 2.8: Circumferential moment a05Rg07.

Table 2.1: Optimal values of parameters.

V_0	α	γ	W_o	W_*	e
0.45	0.490363	0.275881	$4.38282 \cdot 10^{-6}$	$5.15278 \cdot 10^{-6}$	0.85057
0.50	0.549226	0.284027	$3.86136 \cdot 10^{-6}$	$4.6375 \cdot 10^{-6}$	0.83264
0.55	0.605052	0.290123	$3.46249 \cdot 10^{-6}$	$4.21591 \cdot 10^{-6}$	0.82129
0.60	0.658147	0.294337	$3.15763 \cdot 10^{-6}$	$3.86458 \cdot 10^{-6}$	0.81707
0.65	0.708775	0.296677	$2.92554 \cdot 10^{-6}$	$3.56731 \cdot 10^{-6}$	0.82010
0.70	0.757151	0.296968	$2.74998 \cdot 10^{-6}$	$3.3125 \cdot 10^{-6}$	0.83018
0.75	0.803436	0.294764	$2.61823 \cdot 10^{-6}$	$3.09167 \cdot 10^{-6}$	0.84687
0.80	0.847728	0.289161	$2.5201 \cdot 10^{-6}$	$2.89844 \cdot 10^{-6}$	0.86947
0.85	0.890033	0.278294	$2.44735 \cdot 10^{-6}$	$2.72794 \cdot 10^{-6}$	0.89714
0.90	0.930189	0.257875	$2.39317 \cdot 10^{-6}$	$2.57639 \cdot 10^{-6}$	0.92888
0.95	0.967623	0.21513	$2.35191 \cdot 10^{-6}$	$2.44079 \cdot 10^{-6}$	0.96358
0.99	0.99431	0.118785	$2.32495 \cdot 10^{-6}$	$2.34217 \cdot 10^{-6}$	0.99265

It is worthwile to mention that the shear force must be continuous for $r \in [0, R]$. However, the function $P = P(r)$ can be discontinuous. In the particular case when $P(r) = const$ instead of (2.21) one has for $r \in [0, R]$

$$Q = -\frac{Pr}{2} \tag{2.22}$$

where the symmetry $Q(0) = 0$ has taken into account.

Substitution of equations (2.5) and (2.21) in (1.1) leads to linear differential equation

$$\frac{dM_1}{dr} + \frac{2M_1}{r} = \frac{M_{0j}}{r} - \frac{1}{r}\int Prdr + C_1 \tag{2.23}$$

for $r \in (0, a)$. In order to find the general solution for equation (2.23) let us first consider the corresponding homogeneous equation. Evidently, the general solution of it has the form

$$M_h = \frac{C}{r^2}. \tag{2.24}$$

The method of variation of the constant in equations (2.23), (2.24) yields

$$C(r) = \frac{M_{00}r^2}{2} - \int \left(r \cdot \frac{Pr^2}{2}\right) dr + \frac{C_1 r}{3} + C_2. \tag{2.25}$$

Thus the radial bending moment in a plastic region $(0, a)$ is defined as

$$M_1 = \frac{M_{00}}{2} - \frac{1}{r^2}\int \frac{Pr^3}{2}dr + \frac{C_1}{3r} + \frac{C_2}{r^2} \tag{2.26}$$

Integration constants C_1, C_2 in equation (2.26) can be determined using the continuity requirements of M_1 at the boundary conditions. If, for instance, the plastic region is located near the center of the plate for $r \in [0, \eta R]$ where $\eta < 1$ then evidently $C_1 = C_2 = 0$. Otherwise the moment M_1 is not limited. Thus in this case

$$M_1 = \frac{M_{00}}{2} - \frac{Pr^2}{8}. \tag{2.27}$$

Here M_{00} denotes the limit moment for the portion of the plate with thickness h_0. The circumferential moment can be found according to equations (2.5), (2.27) as

$$M_2 = \frac{M_{00}}{2} + \frac{Pr^2}{8}. \tag{2.28}$$

2.6 Elastic plastic solution in the case of diamond condition

During the subsequent increasing the load intensity the plate is divided into elastic and plastic regions. Plastic deformations occur in the central part of the plate with radius y. However, the outward part of the plate remains elastic. The deflection in elastic region is defined by equation (2.9) and moments by equation (2.10). Here one has to take $j = 0$, if $r \in [y, R]$.

In the central plastic region the stress profile lies on the yield curve. Principal moments are defined by equations (2.27), (2.28).

For determination of the unknown constants A, B, A_{20}, A_{30}, A_{40} and y, one can use the boundary conditions (2.12) and the continuity conditions at $r = y$

$$\begin{aligned} &[W(y)] = 0, \\ &[M_1(y)] = 0, \\ &\left[\frac{dW(y)}{dr}\right] = 0, \\ &[M_2(y)] = 0. \end{aligned} \tag{2.29}$$

Making use of the second and forth continuity condition in system (2.29) one can determine the constants

$$A_{20} = -\frac{Py^2(\nu + 1) + 4M_0}{16D_0(1 + \nu)} \tag{2.30}$$

and

$$A_{30} = \frac{Py^4(\nu + 1)}{16D_0(\nu - 1)}. \tag{2.31}$$

From the third continuity condition in system (2.29) one can express constant

$$A = \frac{Py^2(\nu+1) - 4M_0}{16D_0(\nu^2-1)}. \tag{2.32}$$

For determining the constant

$$\begin{aligned} A_{40} = {} & \frac{1}{64D_0(\nu^2-1)} \left\{4R^2(\nu-1)[Py^2(\nu+1)+4M_0]\right. \\ & \left. -4(\nu+1)^2y^4P\ln R - PR^4(\nu^2-1)\right\} \end{aligned} \tag{2.33}$$

one can use the second boundary condition from equations (2.12). Making use of the first continuity condition in system (2.29) one can find the constant

$$\begin{aligned} B = {} & \frac{Py^4[(\nu+1)\ln y - \nu]}{16D_0(\nu-1)} + \frac{1}{64D_0(\nu^2-1)} \left\{4R^2(\nu-1)\right. \\ & \left. \cdot[Py^2(\nu+1)+4M_0] - 4(\nu+1)^2y^4P\ln R + P(\nu^2-1)(y^4-R^4)\right\}. \end{aligned} \tag{2.34}$$

Finally, for expressing the constant y one can substitute the constants A_{20} (2.30)and A_{30} (2.31) into the first boundary condition from equations (2.12). This leads to the equation

$$P(\nu+1)y^4 - 2(\nu+1)PR^2y^2 - 8M_0R^2 + PR^4(3+\nu) = 0. \tag{2.35}$$

It is easy to solve the biquadratic equation (2.35) and get the constant

$$y = \sqrt{R^2 \pm \sqrt{\frac{-2R^2(PR^2-4M_0)}{P(\nu+1)}}}. \tag{2.36}$$

2.7 Elastic plastic bending of an annular plate

Elastic plastic deformations of an annular plate with radii a and R will be studied. The plate is subjected to the distributed transverse loading of intensity $P = P(r)$, where r is the current radius. Assume that the outer edge is simply supported whereas the inner edge of the plate is completely free. Therefore, at the outer edge the transverse deflection W and the radial bending moment M_1 must vanish. The radial bending moment is zero at the inner edge, as well. Thus, the boundary conditions are at the outer edge

$$W(R) = 0, \qquad M_1(R) = 0 \tag{2.37}$$

and at the inner edge

$$M_1(a) = 0, \qquad Q(a) = 0 \tag{2.38}$$

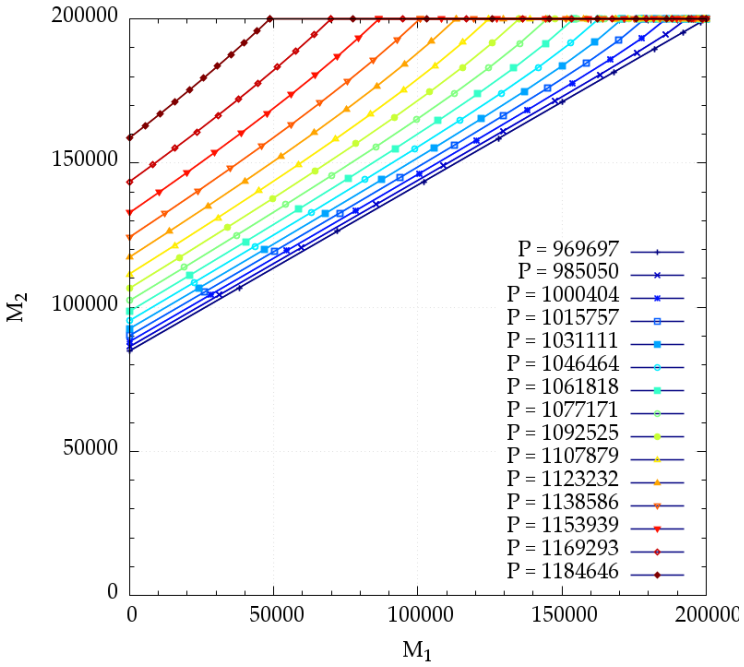

Figure 2.9: Bending moments, Tresca.

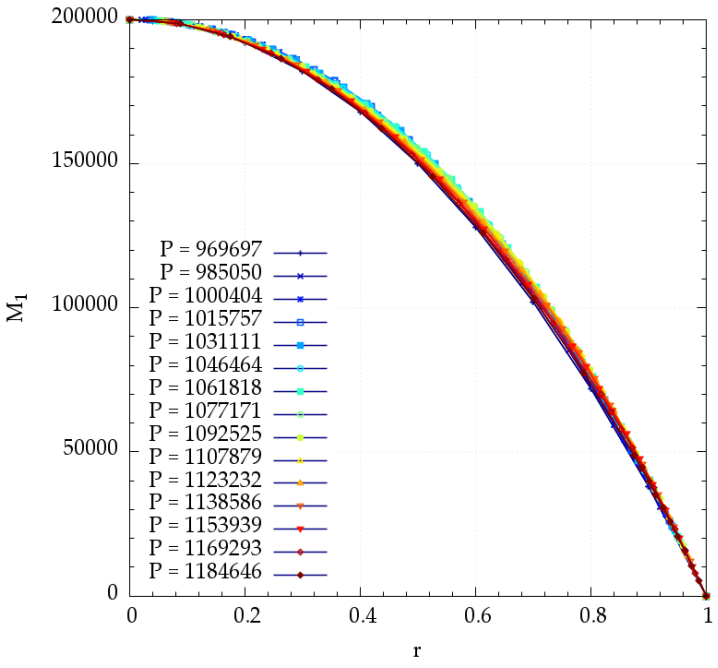

Figure 2.10: Bending moment M_1, Tresca.

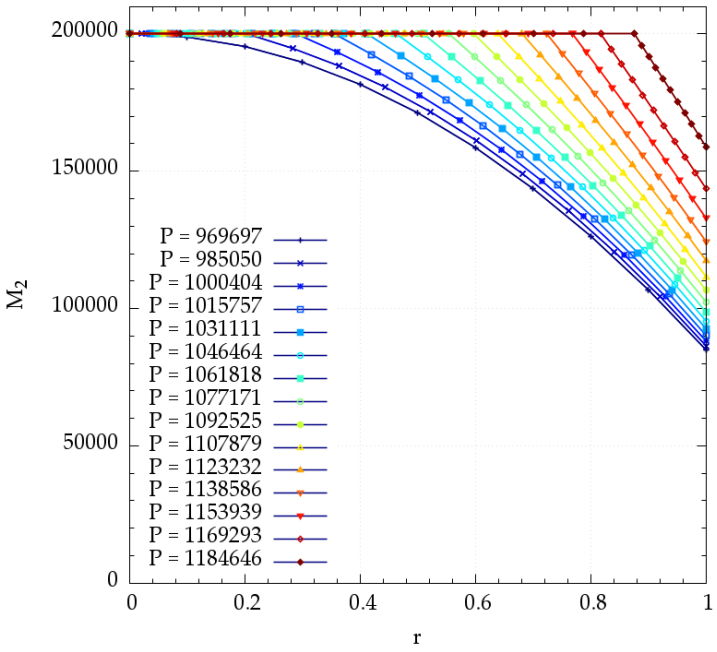

Figure 2.11: Circumferential moment M_2, Tresca.

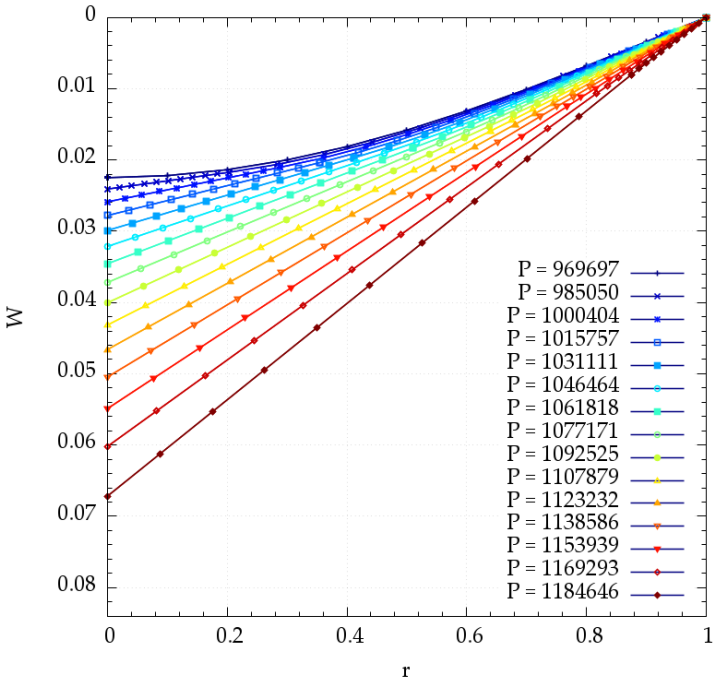

Figure 2.12: Deflection W, Tresca.

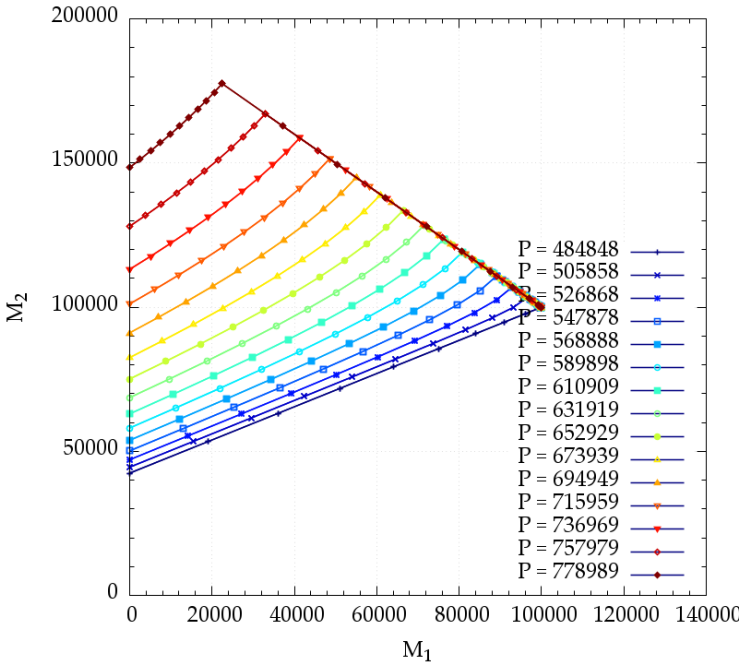

Figure 2.13: Bending moments, diamond.

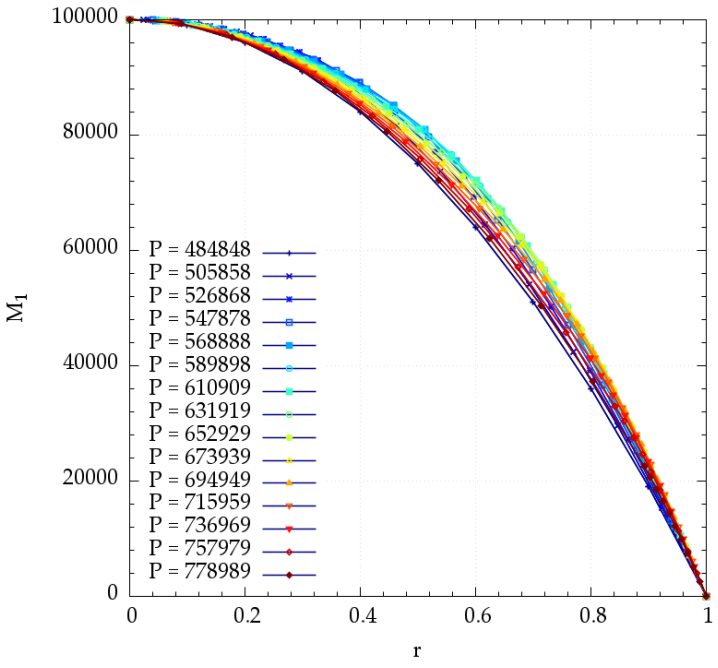

Figure 2.14: Bending moment M_1, diamond.

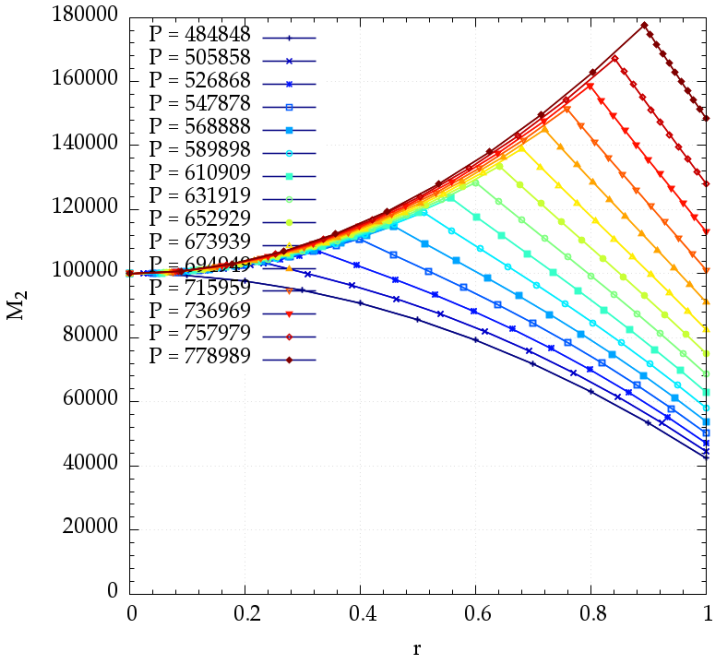

Figure 2.15: Circumferential moment M_2, diamond.

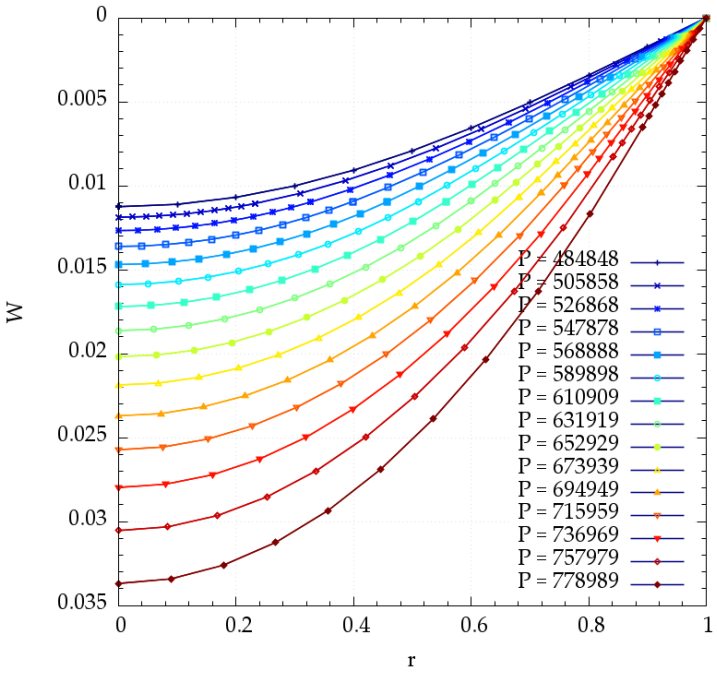

Figure 2.16: Deflection W, diamond.

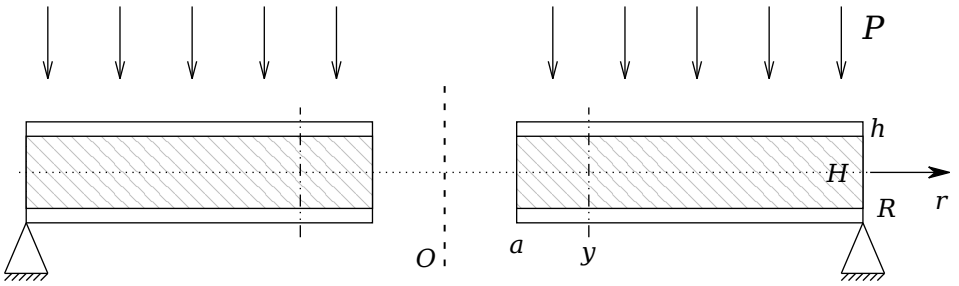

Figure 2.17: Cross-section.

where Q is the shear force. Note that the hoop moment M_2 can take arbitrary values at the both edges. For the sake of simplicity it is assumed that the cross sections of the plate are of sandwich type. Thus the plate consists of two rims of thickness and of the core material between them. Let the total thickness of the plate be H. The aim of the paper is to determine the distributions of bending moments M_1, M_2 and the transverse deflection W for each value of the transverse load. It is expected that in the range of low loadings the plate is fully elastic and with the subsequent increase of the load level elastic plastic deformations occur.

2.7.1 Elastic stage of deformation

In the case of low stress level the plate remains elastic and the Hooke's law holds good. The latter can be presented as (see Reddy [7], Hodge [3]) as in Eq. (1.8). The stresses are coupled with external loads by the equilibrium equations (Save et al [8])

$$\frac{d}{dr}(rM_1) - M_2 - rQ = 0 \tag{2.39}$$

and

$$\frac{d}{dr}(rQ) = -P(r)r. \tag{2.40}$$

In the present case it is assumed that $P(r) = const$. This admits to integrate the last equation. The solution of Eq. 2.40 satisfying the boundary condition (2.38) can be presented as

$$Q = -\frac{P(r^2 - a^2)}{2r}. \tag{2.41}$$

The general solution of Eq. (1.14) satisfying (2.37) is

$$W = \frac{P(r^4 - R^4)}{64D} + A_1(r^2 \ln r - R^2 \ln R) + A_2(r^2 - R^2) + A_3 \ln \frac{r}{R} \tag{2.42}$$

A_1 – A_3 being arbitrary constants. However, calculating the shear force Q from (2.39) making use of (1.11), (1.8), (2.42) and comparing with (2.41) one can see that

$$A_1 = -\frac{Pa^2}{8D} \tag{2.43}$$

Substituting (2.42) in Eq. (1.11) one can determine the bending moments

$$\begin{aligned} M_1 = &-\frac{Pr^2(3+\nu)}{16} + \frac{Pa^2[2(1+\nu)\ln r + 3 + \nu]}{8} \\ &-D\left[2A_2(1+\nu) + \frac{A_3(\nu-1)}{r^2}\right] \end{aligned} \tag{2.44}$$

and

$$\begin{aligned} M_2 = &-\frac{Pr^2(1+3\nu)}{16} + \frac{Pa^2[2(1+\nu)\ln r + 1 + 3\nu]}{8} \\ &-D\left[2A_2(1+\nu) + \frac{A_3(1-\nu)}{r^2}\right]. \end{aligned} \tag{2.45}$$

Applying the boundary conditions (2.37), (2.38) to Eq. (2.44) one can define

$$\begin{aligned} A_2 = &\frac{P}{32D(1+\nu)(R^2-a^2)} \cdot \big\{(3+\nu)(a^4-R^4) \\ &+2a^2[(R^2-a^2)[2(1+\nu)\ln a + 3 + \nu] - 2R^2(1+\nu)(\ln a - \ln R)]\big\}, \end{aligned} \tag{2.46}$$

$$A_3 = \frac{Pa^2R^2[(3+\nu)(R^2-a^2) + 4a^2(1+\nu)(\ln a - \ln R)]}{16D(\nu-1)(R^2-a^2)}. \tag{2.47}$$

2.7.2 Elastic plastic stage of deformation

The plate remains pure elastic until the stress profile lies entirely inside the Tresca's yield hexagon (Fig. 1.3). During the elastic stage the inequalities

$$|M_1| \le M_0, \qquad |M_2| \le M_0, \qquad |M_1 - M_2| \le M_0 \tag{2.48}$$

are satisfied as strict inequalities. The elastic plastic stage begins at the load level $P = P_1$ when the stress profile reaches to the yield locus. The analysis shows that the stress profile reaches to the side $M_2 = M_0$ of the yield hexagon. The maximum of the hoop moment is achieved at the inner edge of the plate and the quantity P_1 can be calculated from the equation $M_2(a) = M_0$. Therefore,

$$P_1 = \frac{8M_0(R^2-a^2)}{R^4(3+\nu) + 4a^2R^2[(1+\nu)(\ln a - \ln R) - 1] + a^4(1-\nu)}. \tag{2.49}$$

During the elastic plastic stage the plate is divided into two parts. In the inner part (a, y) plastic deformations take place whereas the region (y, R) remains elastic. Let us consider the regions separately.

Plastic region, $r \in (a, y)$

For $r \in (a, y)$ the stress profile lies on the side $M_2 = M_0$ of the yield hexagon (Fig. 1.3). Substituting $M_2 = M_0$ in Eq. (2.39) and taking Eq. (2.41) into account one obtains for $r \in (a, y)$

$$rM_1 - rM_0 + \frac{P}{2}\left(\frac{r^3}{3} - a^2 r\right) = C, \tag{2.50}$$

C being an arbitrary constant. Due to the boundary condition (2.38)

$$C = -aM_0 - \frac{Pa^3}{3} \tag{2.51}$$

and Eq. (2.50) can be put into the form

$$M_1 = \frac{r-a}{r}\left[M_0 - \frac{P(r^2 + ar - 2a^2)}{6}\right]. \tag{2.52}$$

It is worthwhile to emphasize that Eq. (2.52) holds good for $r \in (a, y)$. The deflection W is expressed by the formula (1.23).

Elastic region, $r \in (y, R)$

In the elastic region of the plate the relations (2.42) – (2.45) hold good. However, Eq. (2.46) and (2.47) are not valid. For determination of unknown constants A_2, A_3 and A, B one can use the boundary conditions at $r = y$, also the continuity requirements of quantities W, $\dfrac{dW}{dr}$, M_1, M_2 at $r = y$. The requirements $M_1(R) = 0$ and $M_2(y) = M_0$ give with the help of Eq. (2.44), (2.45)

$$\begin{aligned} &-\frac{PR^2(3+\nu)}{16} + \frac{Pa^2[2(1+\nu)\ln R + 3 + \nu]}{8} \\ &-D\left[2A_2(1+\nu) + \frac{A_3(\nu-1)}{R^2}\right] = 0 \end{aligned} \tag{2.53}$$

and

$$\begin{aligned} &-\frac{Py^2(1+3\nu)}{16} + \frac{Pa^2[2(1+\nu)\ln y + 1 + 3\nu]}{8} \\ &-D\left[2A_2(1+\nu) + \frac{A_3(1-\nu)}{y^2}\right] = M_0. \end{aligned} \tag{2.54}$$

The continuity of the radial bending moment at $r = y$ with Eq. (2.44) and (2.52) furnishes the relation

$$\begin{aligned} &\frac{Pa^2[2(1+\nu)\ln y + 3 + \nu]}{8} - D\left[2A_2(1+\nu) + \frac{A_3(\nu-1)}{y^2}\right] \\ &-\frac{Py^2(3+\nu)}{16} - \frac{y-a}{y}\left[M_0 - \frac{P(y^2 + ay - 2a^2)}{6}\right] = 0. \end{aligned} \tag{2.55}$$

Due to the continuity of the deflection and its slope one has making use of Eq. (2.42) and (1.23)

$$A = \frac{Py^3}{16D} - \frac{Pa^2y(2\ln y)+1}{8D} + 2A_2y + \frac{A_3}{y} \tag{2.56}$$

and

$$\begin{aligned} &-\frac{P(y^4-R^4)}{64D} - \frac{Pa^2(y^2\ln y - R^2\ln R)}{8D} + A_2(y^2-R^2) \\ &+A_3\ln\frac{y}{R} - Ay - B = 0. \end{aligned} \tag{2.57}$$

From Eq. (2.55), (2.54) one can easily define

$$\begin{aligned} A_2 = &\frac{1}{48D(1+\nu)y}\cdot\{-Py^3(1+3\nu) + 6Pa^2y[(\nu+1)\ln y + \nu] \\ &+12M_0(a-2y) + 4Pa^3\} \end{aligned} \tag{2.58}$$

and

$$A_3 = \frac{y[Py^3(1+3\nu) - 6Pa^2y(1+\nu) + 8a(3M_0+Pa^2)]}{48D(\nu-1)}. \tag{2.59}$$

The equation (2.57) admits to define

$$\begin{aligned} B = &\frac{P[-3y^4 + 8a^2y^2(\ln y + 1) - R^2(R^2 - 8a^2\ln R)]}{64D} \\ &-(y^2+R^2)A_2 + \left(\ln\frac{y}{R} - 1\right)A_3. \end{aligned} \tag{2.60}$$

Substituting A_2, A_3 from Eq. (2.58), (2.59) in (2.53) one obtains the equation

$$\begin{aligned} &-\frac{PR^2(3+\nu)}{16D} + \frac{Pa^2[2(1+\nu)\ln R + 3 + \nu]}{8D} + \frac{1}{24Dy} \\ &\cdot\{-Py^3(1+3\nu) + 6Pa^2y[(\nu+1)\ln y + \nu] + 12M_0(a-2y) + 4Pa^3\} \\ &+\frac{y[Py^3(1+3\nu) - 6Pa^2y(1+\nu) + 8a(3M_0+Pa^2)]}{48DR^2} = 0. \end{aligned} \tag{2.61}$$

The equation (2.61) serves for determination of the quantity y for fixed load intensity P.

2.7.3 Numerical results

The equation (2.61) is solved numerically making use of the computer code *Mathematica*. The results of calculations are presented in Table 2.7.3 and Fig. 2 – Fig. 4 in

Table 2.2: Loading and y.

$P(Pa)$	611197	657220	703243	749266	795289	841312	887335	933358	979381	1025404	1071427
$y(m)$	0.3	0.3245	0.3536	0.3884	0.4304	0.4808	0.5409	0.6115	0.6939	0.7941	0.9989

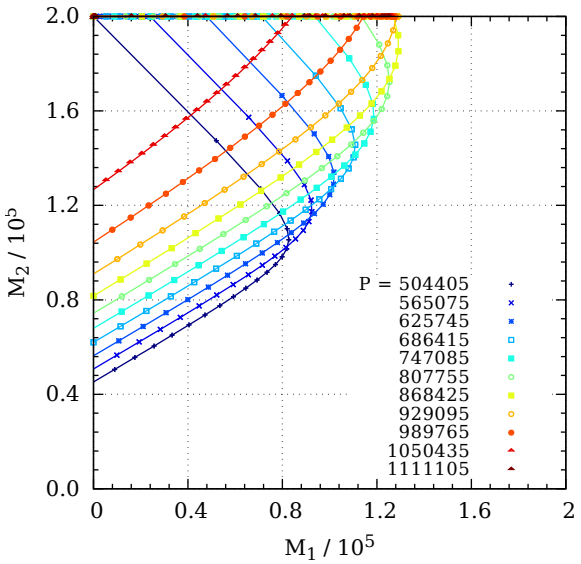

Figure 2.18: Bending moments, annular.

the case $a = 0.3R$. Calculations carried out showed that the plastic region expands with the growth of the load intensity (Table 1).

The transverse deflections of the plate are depicted in Fig. 2 for different values of the load intensity. The enlarged symbols in Fig. 2 indicate the border between elastic and plastic regions. The distributions of bending moments and are presented in Fig. 3 and Fig. 4, respectively. It can be seen from Fig. 3, 4 that the distributions of bending moments are statically admissible since at each corresponding values of , are such that the point either lies on the side of the yield hexagon or is located inside the hexagon. The elastic plastic stage of deformation is completed at the loading level where the whole plate is plastic. This situation corresponds to and .

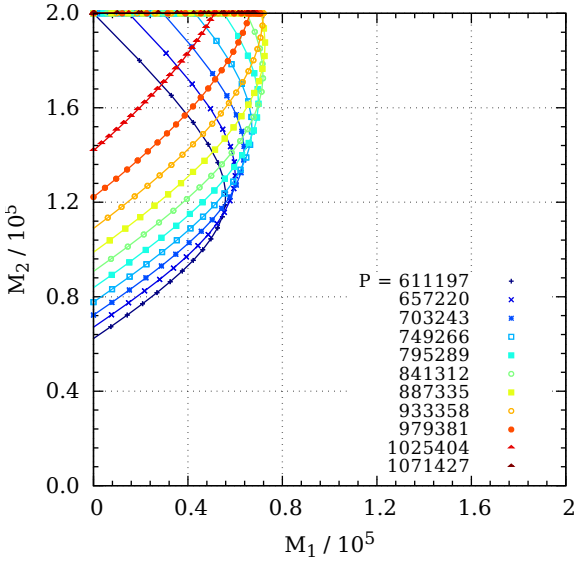

Figure 2.19: Bending moments, annular.

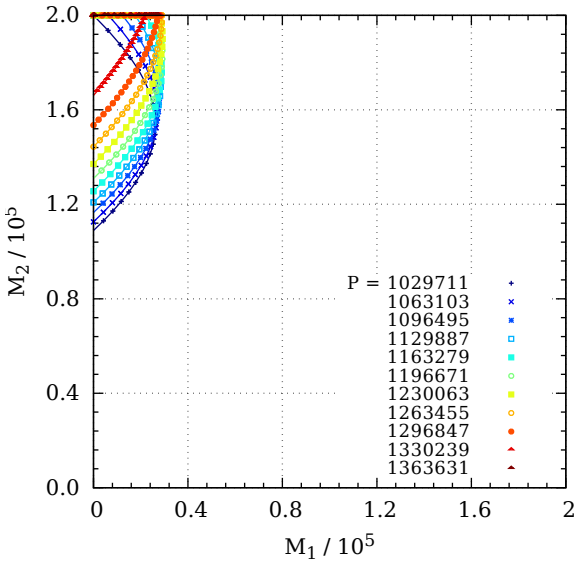

Figure 2.20: Bending moments, annular.

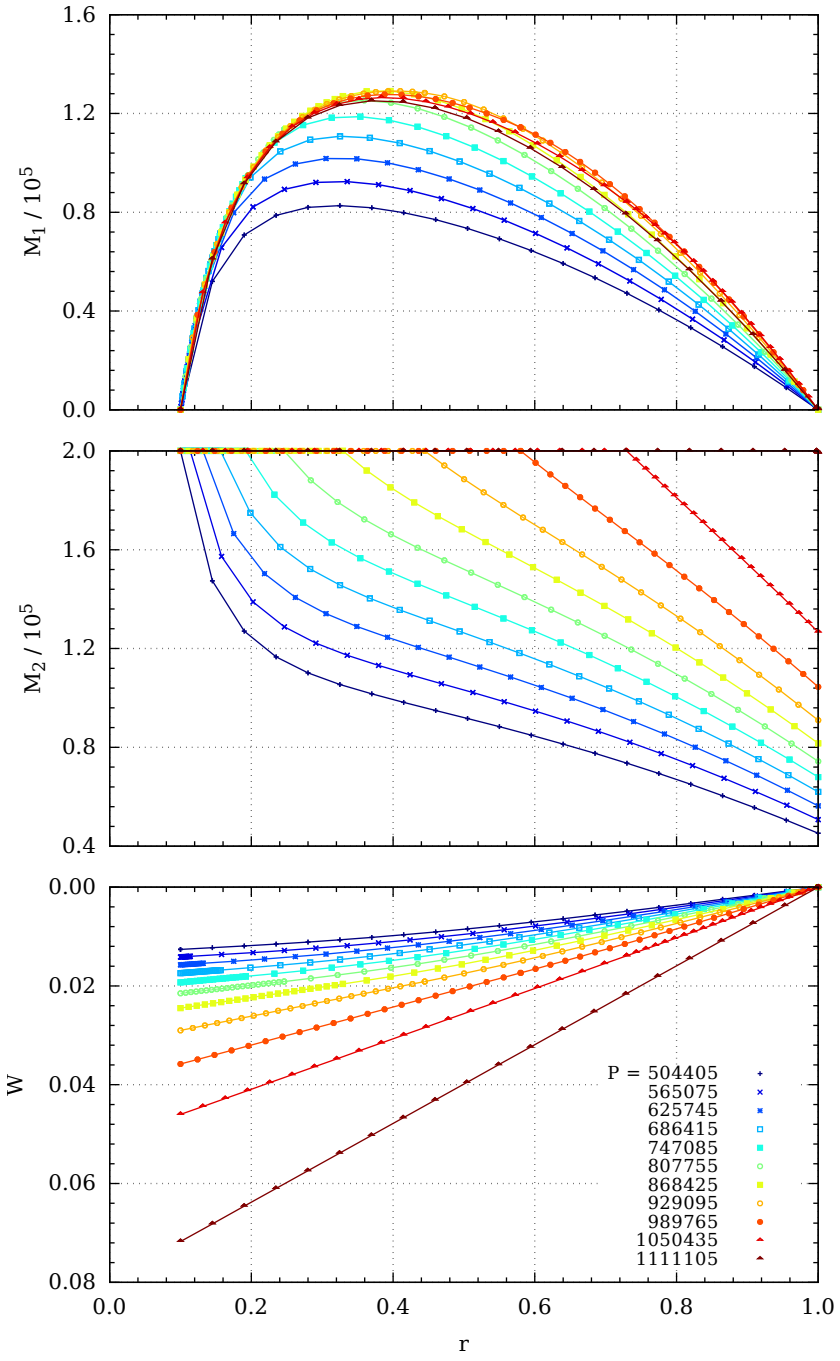

Figure 2.21: Bending moments, annular.

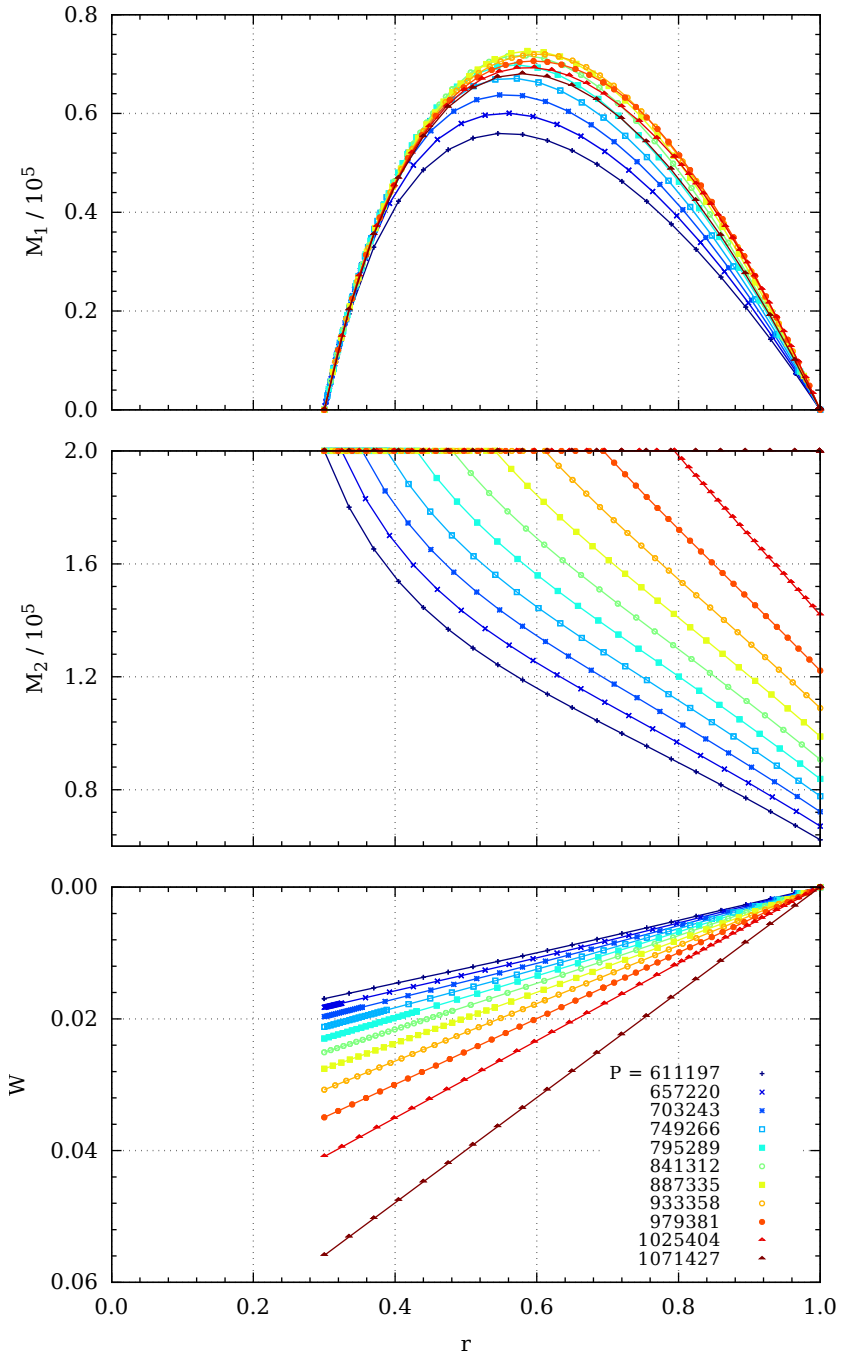

Figure 2.22: Deflection W, annular.

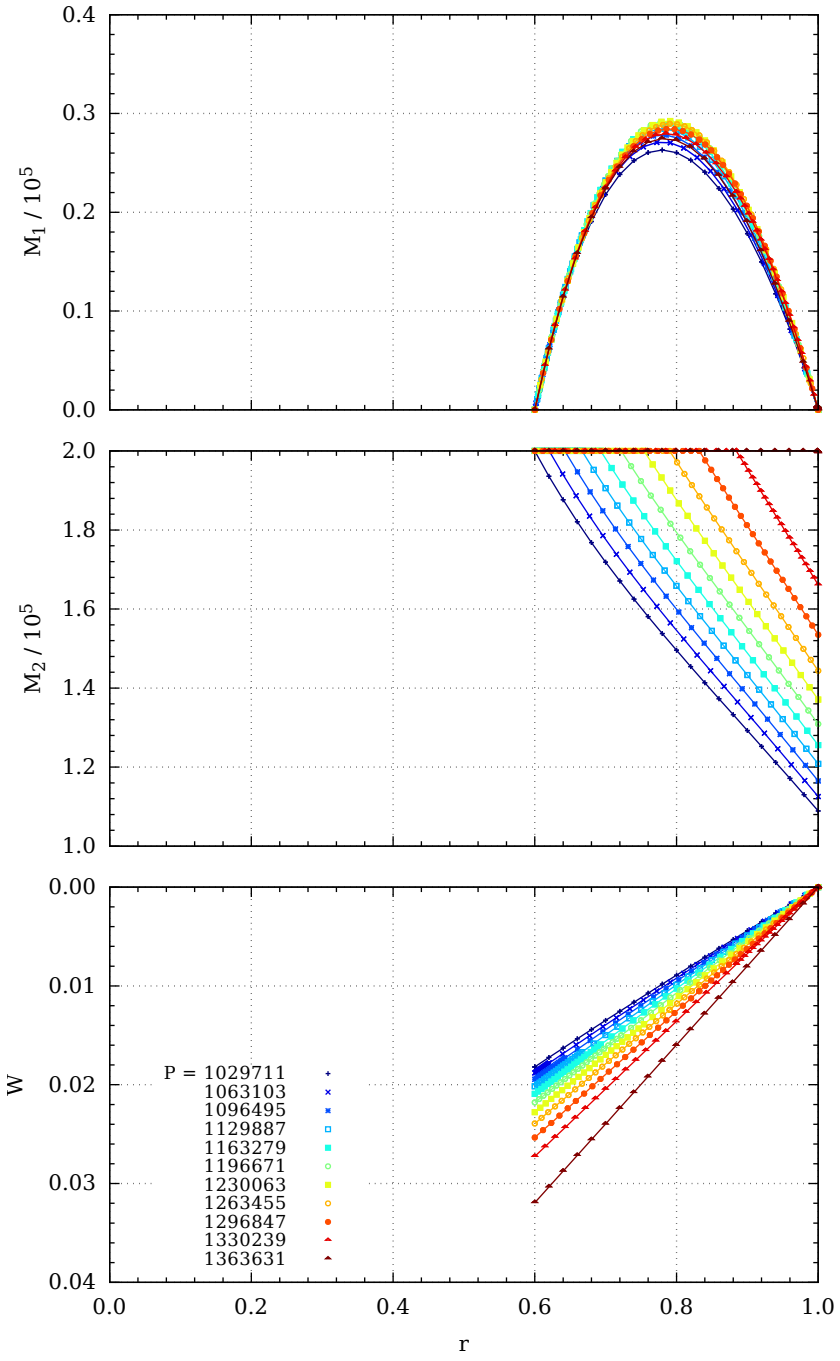

Figure 2.23: Deflection W, annular.

CHAPTER 3
ELASTIC PLASTIC BENDING OF STEPPED ANNULAR PLATES

3.1 Problem formulation and basic hypothesis

Let us consider the axisymmetric bending of an annular plate subjected to the transverse pressure of intensity $P = P(r)$, where r is the current radius. Assume that the internal edge of the plate of radius a is clamped whereas the external edge of radius R is absolutely free. The plate under consideration has sandwich-type cross section (see Fig. 3.1).

The behaviour of the plate will be prescribed with the first order bending theory of thin plates corresponding to small deformations and small displacements (see [32, 41]. The stress state is defined by bending moments M_1, M_2 in the radial and circumferential direction, respectively. Note that the membran forces will be neglected according to current approach. The third generalized stress component to be taken into account is the shear force Q but this component does not contribute to the strain energy when the bending theory is used. Moreover, the shear force, although appearing in the equilibrium conditions, can be eliminated from the equilibrium equations and thus does not involve in the set of governing equations.

As regards kinematical quantities the only displacement to be taken into account is the transverse deflection $W = W(r)$ whereas the radial displacement can be ignored according to the current approach. The strain components corresponding to the generalized stress components M_1, M_2 are the curvature components $\varkappa_1$, $\varkappa_2$ in the radial and circumferential direction, respectively.

It is assumed that the stress strain state induced by the axisymmetric transverse pressure is axisymmetric at each stage of the pressure. Thus the stress and strain components are defined at each point of the plate by the current radius and the given pressure level.

Material of the plate is assumed to be an ideal elastic plastic material obeying the square yield condition in the plastic (inelastic) stage of deformation.

The aim of the chapter is to determine the transverse deflection as well as bending moments distributions in the elastic and subsequent inelastic stages of deformation for given transverse pressure levels.

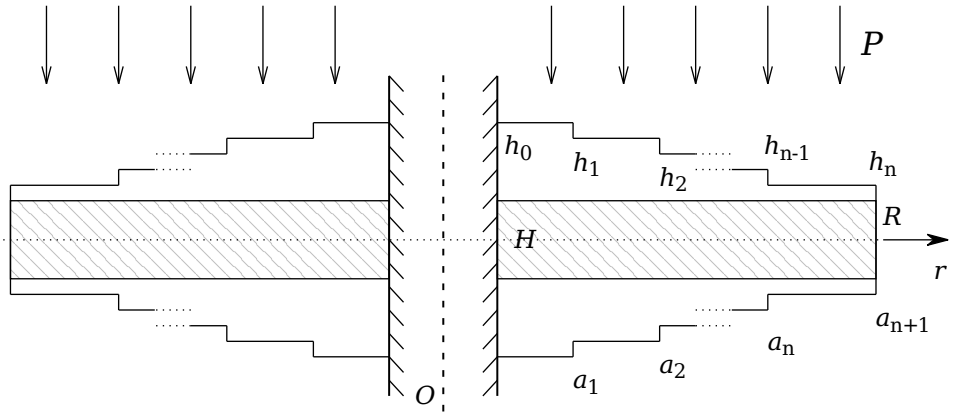

Figure 3.1: Cross-section.

3.2 Basic equations and concepts

It is well known that in the case of lower values of the pressure loading the plate is pure elastic. The elastic behaviour of the material can be prescribed with Hooke's law. The latter is to be presented in the generalized form as

$$\begin{aligned} M_1 &= D_j(\varkappa_1 + \nu\kappa_2), \\ M_2 &= D_j(\varkappa_2 + \nu\kappa_1) \end{aligned} \tag{3.1}$$

where $j = 0, 1$ and in the case of sandwich plate D_j is presented by the formula (2.8).

During the subsequent quasistatic increasing the external loading constitutive equations (3.1) hold good until the elastic limit is exhausted at an unknown point of the plate. In the case of the pressure of constant intensity the yield limit is reached at first at the center of the plate. After that the plate is subdivided into elastic and plastic regions, respectively. Let these regions be S_e and S_p, respectively. Since we are studying the plate of sandwich type and the carrying layers are thin no elastic plastic state of deformatons occurs.

Assume that the material of the plate obeys the square yield condition and associated flow rule (Fig. 3.2). Thus for $r \in S_p$ the stress state of the point is such that the point $(M_1(r),\, M_2(r))$ lies on a side of the square (Fig. 3.2). It means that at each point of the plate are satisfied inequalities

$$|M_1| \le M_{0j}, \qquad |M_2| \le M_{0j} \tag{3.2}$$

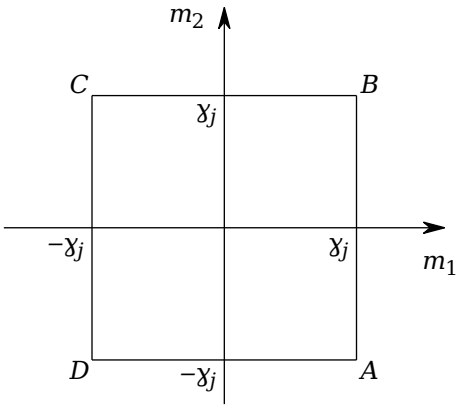

Figure 3.2: Square yield condition.

where M_{0j} stands for the yield moment corresponding to the thickness h_j. It can be easily stated that M_{0j} is presented in form (2.4).

Evidently, at the boundary of the plate requirements

$$\begin{aligned} &M_1(R) = 0, \\ &Q(r) = 0 \end{aligned} \tag{3.3}$$

and

$$W(a) = 0 \tag{3.4}$$

must be satisfied at each loading level.

Let us consider the governing equations separately in elastic and plastic regions, respectively. In elastic regions the stress strain state is determined according to (1.1) and (3.1). Substituting (3.1) and (1.8) in (1.1) easily leads to the equation (2.7).

In the following it is reasonable to use non-dimensional quantities

$$\begin{aligned} &\rho = \frac{r}{R}, \qquad m_1 = \frac{M_1}{M_*}, \qquad m_2 = \frac{M_2}{M_*}, \qquad q = \frac{RQ}{M_*}, \\ &\alpha = \frac{a}{R}, \qquad \alpha_j = \frac{a_j}{R}, \qquad p = \frac{PR^2}{M_*}, \qquad w = \frac{W}{H}, \\ &\gamma_j = \frac{h_j}{h_*}, \qquad d_j = \frac{EH^2 h_j}{2(1-\nu^2)\sigma_0 R^2 h_*} \end{aligned} \tag{3.5}$$

where $M_* = \sigma_0 h_* H$ is the yield moment of a reference plate of constant thickness h_*.

Making use of variables (3.5) one can present the equilibrium equations (1.1) as

$$((\rho m_1)' - m_2)' + p\rho = 0 \tag{3.6}$$

where prims denote the differentiation with respect to the non-dimensional radius ρ.

3.3 General solutions in elastic and plastic regions

Let us denote an elastic region (a_j, a_{j+1}) where the thickness of carrying layers is h_j by S_{ej}.

Making use of (2.7) and (3.5) it is easy to recheck that the general solution of (2.7) can be presented as

$$w = A_{1j}\rho^2 \ln\rho + A_{2j}\rho^2 + A_{3j}\ln\rho + A_{4j} + \frac{p\rho^4}{64 d_j} \tag{3.7}$$

where $\rho \in S_{ej}$ and $d_j = \dfrac{D_j H}{M_* R^2}$. Arbitrary constants $A_{1j}, \dots A_{4j}$ will be determined from the boundary requirements and continuity conditions for w, w', m_1 at the boundaries between elastic and plastic regions.

Non-dimensional bending moments can be determined according to (3.1) and (3.5) as

$$\begin{aligned} m_1 &= -d_j\left(w'' + \frac{\nu}{\rho}w'\right), \\ m_2 &= -d_j\left(\frac{w'}{\rho} + \nu w''\right) \end{aligned} \tag{3.8}$$

for $\rho \in S_{ej}$. The terms with derivatives w', w'' in (3.8) can be expressed as

$$w' = A_{1j}(2\rho\ln\rho + \rho) + 2A_{2j}\rho + \frac{A_{3j}}{\rho} + \frac{p\rho^3}{16 d_j} \tag{3.9}$$

and

$$w'' = A_{1j}(2\ln\rho + 3) + 2A_{2j} - \frac{A_{3j}}{\rho^2} + \frac{3p\rho^2}{16 d_j} \tag{3.10}$$

for $\rho \in S_{ej}$.

The third stress component besides bending moments is the shear force. It is reasonable to calculate it from the equilibrium equations (1.1) or (3.6). From (3.6), (1.1) one easily obtains the equation

$$(\rho q)' = -p\rho \tag{3.11}$$

which holds good over the entire plate. The solution of this equation which satisfies the boundary condition $q(1) = 0$ is

$$q = -\frac{p}{2}\left(\rho - \frac{1}{\rho}\right) \tag{3.12}$$

for $\rho \in (\alpha, 1)$.

The solution of basic equations in a plastic region S_p depends on the particular yield regime. It appears that in the present case the stress strain state in a plastic region of the plate corresponds to the sides AD or DC of the square yield condition (Fig. 3.2). Let us consider these yield regimes in a greater detail.

In the case of the yield profile CD one has $m_1 = -\gamma_j$ for $\rho \in S_{pj} \subset (a_j, a_{j+1})$. However, it can be rechecked (see [7, 34]) that this regime can not take place at a region of finite length.

If the stress profile lies on the side AB of the yield square (Fig. 3.2) then $m_2 = -\gamma_j$ and after integration of (3.6) with (3.12) one has

$$m_1 = -\gamma_j - \frac{p}{2}\left(\frac{\rho^2}{3} - 1\right) + \frac{E_j}{\rho} \tag{3.13}$$

for $\rho \in S_{pj}$.

In the case of the yield regime AD one has $\varkappa_1 = 0$ and thus

$$w = A_j\rho + B_j \tag{3.14}$$

for $\rho \in S_{pj}$, where A_j, B_j are arbritrary constants. However, on the side CD of the yield condition (Fig. 3.2) $\varkappa_2 = 0$ and thus $w = const$. This is one of but not the only reason why the regime CD does not take place in a region of finite length.

3.4 The pure elastic stage of deformation (stage I)

As the intensity of the pressure loading is increased from zero, the entire plate is elastic until the stress profile reaches a side of the yield condition. However, during the elastic stage the stress profile lies inside the square $ABCD$ (Fig. 3.2) where $\gamma = \min \gamma_j$.

During this stage of loading the deflection is defined by (3.7), bending moments and the shear force by (3.8) and (3.12), respectively. For determination of unknown constants one can use the boundary conditions $w'(a) = w(a) = 0$, $m_1(1) = 0$ and the continuity requirements

$$\begin{aligned} &[w(\alpha_j)] = 0, \\ &[w'(\alpha_j)] = 0, \\ &[m_1(\alpha_j)] = 0 \end{aligned} \tag{3.15}$$

for $j = 1, \ldots, n$ where the square brackets denote finite jumps, e. g. $[z(\alpha_j)] = z(\alpha_j + 0) - z(\alpha_j - 0)$.

It appears that the general solution in the form (3.7) may involve inadequate solutions for particular cases. In order to avoid this one has to check if the shear force in the form (3.12) concides with that following from the first equation of the system (1.1).

Let us denote

$$\rho\bar{q} = (\rho m_1)' - m_2. \tag{3.16}$$

Evidently, $\bar{q} = q$. Thus one has to check if the constraints

$$\bar{q}(\rho) = q(\rho) \tag{3.17}$$

for $\rho \in S_{ej}$ ($j = 1, \ldots, n$) with the boundary condition $\bar{q}(1) = 0$ are satisfied. Making use of (3.7) - (3.10) and (3.12) with (3.16) it is easy to show that equalities (3.17) take place if

$$A_{1j} = -\frac{p}{8d_j} \tag{3.18}$$

for $j = 0, \ldots, n$.

Thus, for determination of $3n + 3$ unknown constants A_{2j}, A_{3j}, A_{4j} ($j = 0, \ldots, n$) one has three boundary conditions and $3n$ continuity conditions (3.15).

Making use of (3.8), (3.9), (3.10) and taking (3.18) into account it is easy to determine the bending moments

$$\begin{aligned} m_1 = {} & \frac{-p\rho^2(3+\nu)}{16} - \frac{p}{8}[2(1+\nu)\ln\rho + 3 + \nu] \\ & -2(1+\nu)A_{2j}d_j + \frac{A_{3j}d_j(1-\nu)}{\rho^2} \end{aligned} \tag{3.19}$$

and

$$\begin{aligned} m_2 = {} & \frac{-p\rho^2(1+3\nu)}{16} - \frac{p}{8}[2(1+\nu)\ln\rho + 1 + 3\nu] \\ & -2(1+\nu)A_{2j}d_j + \frac{A_{3j}d_j(1-\nu)}{\rho^2} \end{aligned} \tag{3.20}$$

for $\rho \in (a_j, a_{j+1})$, $j = 0, \ldots, n$.

It is interesting to remark that the distribution of the shear force does not depend on the distribution of thicknesses, as it can be seen from (3.12). At the same time other stress components (bending moments) do depend on the thicknesses.

The elastic loading stage completes at the moment when the stress profile reaches the side CD of the yield square. In the case of a plate of constant thickness the plastic

yielding happens at first at the internal edge of the plate for $\rho = \alpha$. At the limit stage between the fully elastic stage and inelastic stage for $p = p_0$

$$m_1(\alpha) = -\gamma_0. \tag{3.21}$$

Note that, in principle, the plastic yielding may start elsewhere, as well. If, for instance, the inner annulus is very narrow and the thickness h_0 is large whereas the next annulus has very small thickness then the yield can start from the next annulus. However, these cases will not studied in the present work.

3.5 Elastic plastic stage with the hinge circle (stage II)

Assume that during this stage of deformation the plastic hinge circle is located at the internal edge of the plate for $\rho \neq \beta$ is elastic as during the previous stage. However, due to the hinge the boundary condition $w'(\alpha) = 0$ is no more valid. For determination of unknown constants A_{2j}, A_{3j}, A_{4j} one can use relations (3.15) – (3.17) with boundary conditions $w(\alpha) = 0$, $m_1(1) = 0$ and (3.21). Note that (3.18) remains valid, as well. The latter admits to present the deflection for $\rho \in [\alpha_j, \alpha_{j+1}]$ as

$$w = \frac{p\rho^2(\rho^2 - 8\ln\rho)}{64d_j} + A_{2j}\rho^2 + A_{3j}\ln\rho + A_{4j}. \tag{3.22}$$

Making use of (3.22), (3.19) and satisfying boundary conditions $w(\alpha) = 0$, $m_1(\alpha) = -\gamma_0$ results in

$$\begin{aligned} &A_{20}\alpha^2 + A_{30}\ln\alpha = -A_{40} - \frac{p\alpha^2(\alpha^2 - 8\ln\alpha)}{64d_0}, \\ &-2A_{20}(1+\nu)d_0 + \frac{d_0(1-\nu)A_{30}}{\alpha^2} \\ &= -\gamma_0 + \frac{p\alpha^2(3+\nu)}{16} + \frac{p[2(1+\nu)\ln\alpha + 3 + \nu]}{8} \end{aligned} \tag{3.23}$$

Finally, employing the continuity conditions (3.15) with boundary conditions (3.23) and $m_1(1) = 0$ admits to determine unknown constants A_{2j}, A_{3j}, A_{4j} for each $j = 0, \ldots, n$.

This stage of determination will be completed when the stress profile at $\rho = \alpha$ reaches the point D (Fig. 3.2) so that $m_2(\alpha) = -\gamma_0$. Let the corresponding value of the external load intensity be p_1.

3.6 The elastic plastic stage with a plastic region of finite length (stage III)

It is reasonabelt to assume that during the subsequent increasing the tansverse pressure plastic deformations take place for $\rho \in S_{p0}$, $\rho \in [\alpha, \eta]$ where η is a previously unknown constant. The plastic region corresponds to the yield regime DA (Fig. 3.2). Thus, for $\rho \in (\alpha, \eta)$

$$m_2 = -\gamma_0. \tag{3.24}$$

The distribution of the radial bending moment m_1 can be calculated by (3.13) taking $j = 0$. As at $\rho = \beta$, $m_1 = -\gamma_0$ the arbitrary constant E_0 is to be

$$E_0 = \frac{\alpha p}{2}\left(\frac{\alpha^2}{3} - 1\right). \tag{3.25}$$

Thus the bending moment is defined as

$$m_1 = -\gamma_0 - \frac{p}{2}\left(\frac{\rho^2}{3} - 1\right) + \frac{\alpha p}{2\rho}\left(\frac{\alpha^2}{3} - 1\right) \tag{3.26}$$

for $\rho \in [\alpha, \eta]$.

The tranverse deflection has the form (3.14) in the plastic region S_{p0}. According to the boundary condition $w(\alpha) = 0$ must be $B_0 = -A_0\alpha$. Thus

$$w = A_0(\rho - \alpha) \tag{3.27}$$

for $\rho \in [\alpha, \eta]$.

Since we can now define $w(\eta)$, $w'(\eta)$, $m_1(\eta)$ the subsequent solution procedure is similar to that accomplished in the previous section. Note that for $\rho > \eta$ the plate is elastic. For determination of the parameter η one has to use the continuity of the moment m_2 taking $m_2(\eta) = -\gamma_0$.

3.7 Several plastic regions

The previous stage of loading terminates at the moment when plastic yielding takes place in the section S_{p1} or in another section. Let us assume for the conceteness sake that the stress profile reaches to the corresponding yield level at $\rho = \alpha_1$ when $p = p_2$. Thus for $p \geq p_2$ the plastic deformations take place in the region (α_1, η_1) as well as in (α, η) which continues the extension. It means that $m_2 = -\gamma_0$ for $\rho \in (\alpha_1, \eta_1)$.

The bending moment distribution for $\rho \in S_{p1}$ can be defined according to (3.13) with the unknown constant E_1. Similarily the deflection w is given by (3.14) with unknown constants A_1, B_1.

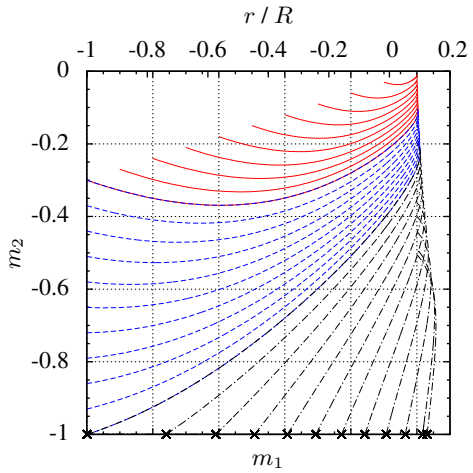

Figure 3.3: Bending moments m_1, m_2.

The procedure of the determination of constants of integration is similar to that accomplished in the previous case. Now we have to take into account that the region (η, α_1) between plastic regions remain elastic. Here we have unknown constants A_{21}, A_{31}, A_{41}. The number of unknowns in each region is, thus, three. For determination of these constants the continuity requirements for m_1, w, w' are applicable. Finally, the parameters η, η_1 are to be determined from equations $m_2(\eta) = -\gamma_0$ and $m_2(\eta_1) = -\gamma_1$ where m_2 is calculated for an elastic region according to (3.20) with previously defined constants A_{2j}, A_{3j}.

3.8 Numerical results

Results of calculations in the case of plates with a single step are presented in Fig. 3.3 – 3.9. The results regard to the plate with inner radius $a = 0.2R$.

The stress profiles on the plane of moments m_1, m_2 are shown in Fig. 3.3 for different values on the load intensity. It can be seen from Fig. 3.3 that the profiles corresponding to smaller values of the load p lie wholly inside the square $|m_1| \leq 1$, $|m_2| \leq 1$. When the load intensity increases until $p = p_1$ the end of the profile reaches the side $m_1 = -1$ and for $p = p_2$ the corner point where $m_1 = m_2 = -1$. During subsequent growth of the load intensity the end of the stress profile lies on the side $m_2 = -1$ as it was expected theoretically.

Distributions of bending moments m_1 and m_2 are presented in Fig. 3.4 – Fig. 3.6 and Fig. 3.7 – Fig. 3.9, respectively. The locations of boundaries between elastic and

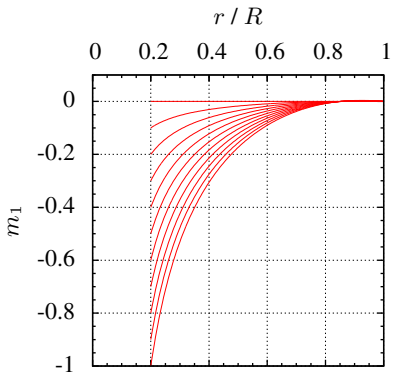

Figure 3.4: Radial bending moment m_1; stage I.

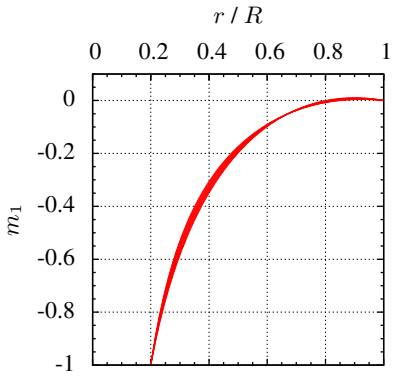

Figure 3.5: Radial bending moment m_1; stage II.

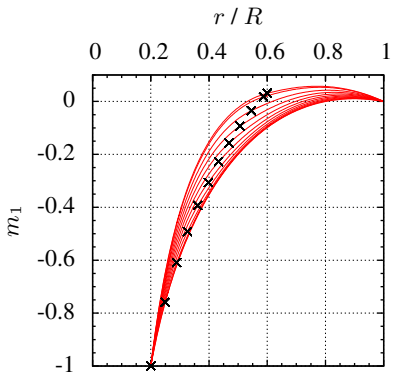

Figure 3.6: Radial bending moment m_1; stage III.

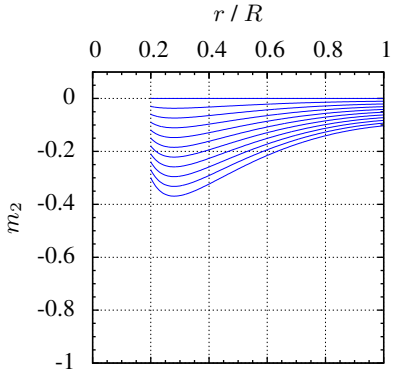

Figure 3.7: Hoop moment m_2; stage I.

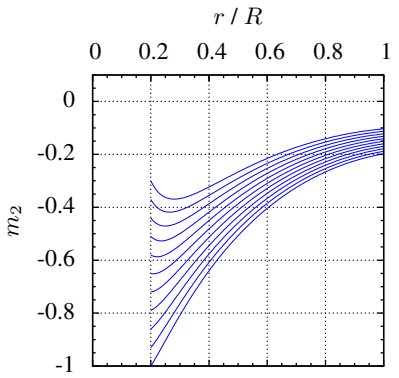

Figure 3.8: Hoop moment m_2; stage II.

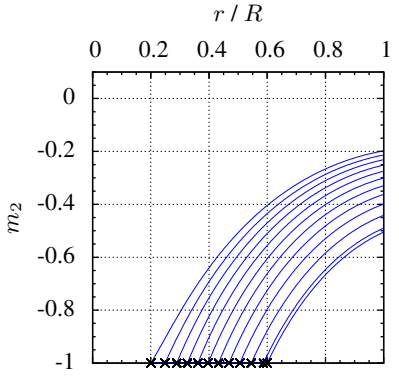

Figure 3.9: Hoop moment m_2; stage III.

plastic regions in Fig. 3.6 are shown by asterisks. It can be seen from Fig. 3.8 that when the load increases the stress state tends to the pure plastic state. In the case of a plate of constant thickness in the pure plastic state $m_2 \equiv -1$. In the case of a stepped plate it can be such that $m_2 = -\gamma_j$ for $\rho \in (\alpha_j, \alpha_{j+1})$, $j = 0, \ldots, n$. However, the question which is the stress state at the plastic collapse can be answered by the limit analysis of the plate of particular shape.

3.9 Concluding remarks

A method for theoretical investigation of axisymmetric plates subjected to the distributed transverse pressure was developed. The material of plates was assumed to be an ideal elastic plastic material obeying the square yield condition and the associated flow law in the range of inelastic deformations. In order to get maximal simplicity of the posed problem hardening of the material as well as geometrical non-linearity of the plate behaviour were neglected.

It was assumed that the plates under consideration had piecewise constant thickness with arbitrary number of steps. Exact solutions were developed for the case when the plate is clamped at the inner edge whereas the outer edge is absolutely free. As a result of the solution procedure a succession of stress states which are in equilibrium with the external loading were constructed that led from the wholly elastic to the elastic plastic state and finally to the plastic collapse state.

CHAPTER 4
OPTIMIZATION OF ELASTIC CIRCULAR PLATES WITH ADDITIONAL SUPPORTS

4.1 Formulation of the problem

The plate under consideration is simply supported at the edge and it is resting on an absolutely rigid ring support of unknown radius $r = s$. From practical considerations it is evident that the desirable position of the additional support is such that the maximal deflection of the plate is as small as possible. Thus the optimal location of the internal support should minimize the functional

$$J_1 = \max_{r\in[0,R)} W(r, P, s) \tag{4.1}$$

for given loading $P = P(r)$ and thickness $h = h(r)$. However, the cost function presented in the form (4.1) has several drawbacks. First of all, it is a non-differentiable and non-additive functional. The use of non-differentiable functionals in the solution of problems of optimization is quite complicated. On the other hand, the functional (4.1) ignores the expenditures necessary for manufacturing of the additional support.

It can be shown that an approximation of the functional (4.1) can be presented as [3, 18]

$$J_2 = \left(\int_0^R W^k r dr\right)^{\frac{1}{k}} \tag{4.2}$$

where k is an integer. If $k \to \infty$ then $J_2 \to \|W\|$.

Due to the circumstancies mentioned above in the present paper the cost function

$$J = \int_0^R W^k r dr + \mu_0 2\pi s \tag{4.3}$$

will be employed. In (4.3) μ_0 stands for the specific cost (cost per unique length) of the additional support. We assume herein that the material cost of the additional support is proportional to its length.

The aim of the chapter is to determine the design of the plate with an additional support (see Fig. 4.1) which minimizes the cost function (4.3) so that at each value of P governing equations of the theory of thin axisymmetric plates with appropriate boundary conditions are satisfied.

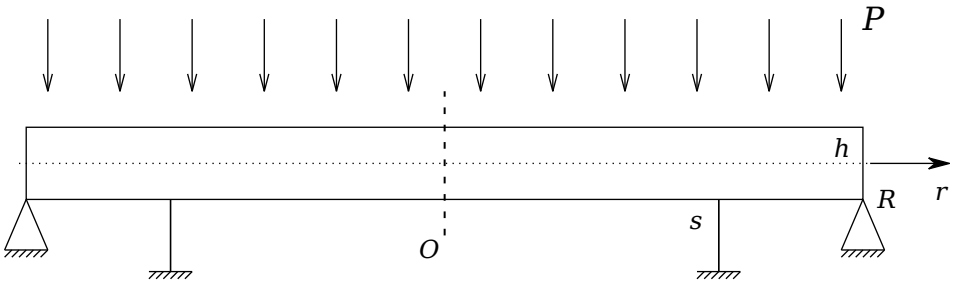

Figure 4.1: Circular plate with additional support.

4.2 Boundary conditions

Taking a look at the equilibrium and constitutive equations (1.1) – (1.9) it appears that one can eliminate from the set of basic equations variables σ_1, ε_1, σ_2, ε_2, κ_1, κ_2 and also M_2. Introducing another new variable Z one can present the system of governing equations as

$$\begin{aligned}
&\frac{dW}{dr} = Z,\\
&\frac{dZ}{dr} = -\frac{M_1}{D} - \frac{\nu Z}{r},\\
&\frac{dM_1}{dr} = \frac{D(\nu^2-1)Z}{r^2} - \frac{M_1(1-\nu)}{r} + Q,\\
&\frac{dQ}{dr} = -\frac{Q}{r} - P(r),
\end{aligned} \tag{4.4}$$

where the flexural stiffness

$$D = \frac{Eh^3}{12(1-\nu^2)}. \tag{4.5}$$

Variables W, Z, M_1, Q will be treated as state variables which satisfy the state equations (4.4) with appropriate boundary and intermediate conditions. At the outer edge of the plate , e. g. at $r = R$ bending moment M_1 and the deflection W must vanish. Thus

$$M_1(R) = 0, \qquad W(R) = 0. \tag{4.6}$$

Due to the symmetry at the center of the plate

$$\frac{dW}{dr}(0) = 0, \qquad Q(0) = 0. \tag{4.7}$$

At $r = s$ where the rigid ring support is located must be

$$W(s) = 0. \tag{4.8}$$

Note that state variables W, Z, M_1 are continuous whereas Q can be discontinuous at $r = s$.

4.3 Necessary optimality conditions

In order to establish the requirements to be satisfied by the optimal solution let us introduce the augmented functional (see Bryson [6], Hull [12]; Lellep, Polikarpus [20])

$$J_* = \mu s + \int_0^s F_* dr + \int_s^R F_* dr \tag{4.9}$$

where according to (4.3), (4.4)

$$\begin{aligned} F_* = W^k &+ \psi_1 \left(\frac{dW}{dr} - Z \right) + \psi_2 \left(\frac{dZ}{dr} + \frac{M_1}{D} + \frac{\nu Z}{r} \right) + \\ &+ \psi_3 \left(\frac{dM_1}{dr} - \frac{D(\nu^2 - 1)Z}{r^2} + \frac{M_1(1-\nu)}{r} - Q \right) + \\ &+ \psi_4 \left(\frac{dQ}{dr} + \frac{Q}{r} + P(r) \right) \end{aligned} \tag{4.10}$$

and $\mu = 2\pi\mu_0$, the quantities $\psi_1 - \psi_4$ being adjoint variables.

Evidently the problem posed above belongs to the class of optimal control problems with moving boundaries. Therefore, one has to employ total variations when deriving necessary conditions of minimum of the functional (4.9). The total variation of a state variable y at $r = s + 0$ or at $r = s - 0$ must be calculated by the following sample

$$\Delta y(s \pm 0) = \delta y(s \pm 0) + \frac{dy(s \pm 0)}{dr} \cdot \Delta s \tag{4.11}$$

where Δy is the total variation and δy stands for the ordinary variation of the variable y. If the state variable is continuous at $r = s$ then, ofcourse, $\Delta y(s - 0) = \Delta y(s + 0) = \Delta y(s)$. However, in the case of discontinuous variables one has to distinguish the quantities $\Delta y(s - 0)$ and $\Delta y(s + 0)$. Note that even in the case of continuous variables the quantities $\delta y(s - 0)$ and $\delta y(s + 0)$ must not be equal to each other.

The total variation of a Lagrange' functional is calculated by the rule (see Bryson [6]),

$$\Delta \int_0^s F dr = \delta \int_0^s F dr + F|_s \cdot \Delta s \tag{4.12}$$

where Δs stands for an arbitrary increment of s. According to (4.12) one can write

$$\Delta J_* = \mu\Delta s + \delta\int_0^s F_* dr + \delta\int_s^R F_* dr + F_*|_{s-}\Delta s - F_*|_{s+}\Delta s. \tag{4.13}$$

Taking (4.10) into account one can easily determine the following weak variation

$$\begin{aligned}
&\delta\textstyle\int_a^b F_* dr = \int_a^b \Big\{ kW^{k-1} r\delta W - \frac{d\psi_1}{dr}\delta W - \psi_1\delta Z - \frac{d\psi_2}{dr}\delta Z + \\
&+\frac{\psi_2}{D}\delta M_1 + \frac{\nu\psi_2}{r}\delta Z - \frac{d\psi_3}{dr}\delta M_1 - \frac{D(\nu^2-1)\psi_3}{r^2}\delta Z + \\
&+\frac{\psi_3(1-\nu)}{r}\delta M_1 - \psi_3\delta Q - \frac{d\psi_4}{dr}\delta Q + \frac{\psi_4}{r}\delta Q \Big\} dr + \\
&+ (\psi_1\delta W + \psi_2\delta Z + \psi_3\delta M_1 + \psi_4\delta Q)\Big|_a^b
\end{aligned} \tag{4.14}$$

where a and b are arbitrary boundaries of integration.

Substituting the both integrals in (4.13) by (4.14) with appropriate choise of boundaries a and b leads to the relation

$$\begin{aligned}
&\Delta J_* = \mu\Delta s + \textstyle\int_0^R \Big\{ kW^{k-1} r\delta W - \frac{d\psi_1}{dr}\delta W - \psi_1\delta Z - \frac{d\psi_2}{dr}\delta Z + \\
&+\frac{\psi_2}{D}\delta M_1 + \frac{\nu\psi_2}{r}\delta Z - \frac{d\psi_3}{dr}\delta M_1 - \frac{D(\nu^2-1)\psi_3}{r^2}\delta Z + \\
&+\frac{\psi_3(1-\nu)}{r}\delta M_1 - \psi_3\delta Q - \frac{d\psi_4}{dr}\delta Q + \frac{\psi_4}{r}\delta Q \Big\} dr + \\
&+ (\psi_1\delta W + \psi_2\delta Z + \psi_3\delta M_1 + \psi_4\delta Q)\,|_0^s + \\
&+ (\psi_1\delta W + \psi_2\delta Z + \psi_3\delta M_1 + \psi_4\delta Q)\,|_s^R
\end{aligned} \tag{4.15}$$

where the matter that $F_*(s) = 0$ has taken into account.

Making use of (4.15) one easily obtains from the equation $\Delta J_* = 0$ the system of adjoint equations

$$\begin{aligned}
&\frac{d\psi_1}{dr} = rkW^{k-1}, \\
&\frac{d\psi_2}{dr} = -\psi_1 + \frac{\nu\psi_2}{r} - \frac{D(\nu^2-1)\psi_3}{r^2}, \\
&\frac{d\psi_3}{dr} = \frac{\psi_2}{D} + \frac{\psi_3(1-\nu)}{r}, \\
&\frac{d\psi_4}{dr} = -\psi_3 + \frac{\psi_4}{r}.
\end{aligned} \tag{4.16}$$

Note that although the adjoint set (4.16) holds good for each $r \in [0, r]$ it must be integrated separately in regions $(0, s)$ and (s, R), respectively. The reason is that some of adjoint variables can be discontinuous at $r = s$.

Boundary conditions (4.6), (4.7) admit to present the transversality conditions as

$$\psi_1(0) = 0, \qquad \psi_3(0) = 0 \tag{4.17}$$

and

$$\psi_2(R) = 0, \qquad \psi_4(R) = 0. \tag{4.18}$$

Substituting (4.16) – (4.18) in (4.15) admits to rewrite the equation $\Delta J_* = 0$ as

$$\mu\Delta s - (\psi_1\delta W + \psi_2\delta Z + \psi_3\delta M_1 + \psi_4\delta Q)|_{s-0}^{s+0} = 0. \tag{4.19}$$

From the physical considerations it is evident that W, Z and M_1 are continuous at $r = s$. Thus following (4.11) one can write

$$\begin{aligned}
\delta W(s \pm 0) &= \Delta W(s) - \frac{dW}{dr}(s) \cdot \Delta s, \\
\delta Z(s \pm 0) &= \Delta Z(s) - \frac{dZ}{dr}(s) \cdot \Delta s, \\
\delta M_1(s \pm 0) &= \Delta M_1(s) - \frac{dM_1(s \pm 0)}{dr} \cdot \Delta s, \\
\delta Q(s \pm 0) &= \Delta Q(s \pm 0) - \frac{dQ(s \pm 0)}{dr} \cdot \Delta s.
\end{aligned} \tag{4.20}$$

Substituting the weak variations of state variables from (4.20) to (4.19) and taking into account that $\Delta W(s) = 0$ and $\Delta Z(s)$, $\Delta M_1(s)$, $\Delta Q(s\pm0)$ are independent leads to the requirements

$$\begin{aligned}
\psi_2(s - 0) - \psi_2(s + 0) = 0, \\
\psi_3(s - 0) - \psi_3(s + 0) = 0
\end{aligned} \tag{4.21}$$

and

$$\psi_4(s - 0) = \psi_4(s + 0) = 0. \tag{4.22}$$

It was assumed above that Z and M_1 are continuous everywhere; thus in particular at $r = s$. Bearing in mind the continuity of M_1 it infers from (1.8) and (1.9) that $\kappa_1 = -\dfrac{dZ}{dr}$ is also continuous at $r = s$.

Substituting (4.20) – (4.22) in (4.19) and taking into account the continuity of Z, κ_1, κ_2 and ψ_2, ψ_3, also the arbitrariness of the increment Δs one can present (4.19) as

$$\mu + [\psi_1(s)]\frac{dW(s)}{dr} + \psi_3(s)\left[\frac{dM_1(s)}{dr}\right] = 0. \tag{4.23}$$

In (4.23) the quadratic brackets denote the finite jumps of corresponding variables at $r = s$, e. g.

$$[y(s)] = y(s + 0) - y(s - 0)$$

where $y(s \pm 0)$ stands for right and left hand limits of the discontinuous variable $y(r)$ at $r = s$.

4.4 Solution of governing equations

Consider the solution of state equations (4.4) in greater detail in the case when the plate thickness h is constant. In this case it follows from (5.16) that $D = const$, as well.

Integrating the last equation in the system (4.4) one obtains

$$Q = -\frac{1}{r}\left(\int P(r)dr + C_{\pm}\right) \tag{4.24}$$

where C_+ and C_- stand for constants of integration in the regions $[0, s]$ and $[s, R]$, respectively. According to formula (1.15) the general solution can be presented as

$$W = \frac{Pr^4}{64D} + A_{1j}r^2 \ln r + A_{2j}r^2 + A_{3j} \ln r + A_{4j} \tag{4.25}$$

for $r \in [r_j, r_{j+1}]$ and $j = 0, 1$. Here the following notation is used: $r_0 = 0$, $r_1 = s$ and $r_2 = R$. Evidently,

$$Z = \frac{Pr^3}{16D} + A_{1j}r(2 \ln r + 1) + 2A_{2j}r + \frac{A_{3j}}{r} \tag{4.26}$$

and

$$\begin{aligned} M_1 &= -\frac{Pr^2(3 + \nu)}{16} - A_{1j}D[3 + \nu + 2(1 + \nu) \ln r] - \\ &-2DA_{2j}(1 + \nu) - \frac{D(\nu - 1)}{r^2}A_{3j}, \\ M_2 &= -\frac{Pr^2(1 + 3\nu)}{16} - A_{1j}D[1 + 3\nu + 2(1 + \nu) \ln r] - \\ &-2DA_{2j}(1 + \nu) - \frac{D(\nu - 1)}{r^2}A_{3j}. \end{aligned} \tag{4.27}$$

The integration constants A_{1j} – A_{4j} will be determined from the boundary and continuity conditions. Let us consider first the solution in the internal region for $r \in [0, s]$.

Here $j = 0$ in (4.25) – (4.27). Since at the center of the plate the quantities $W(0)$, $M_1(0)$, $M_2(0)$ must be finite whereas according to (4.7) $Z(0) = 0$ one has

$$A_{10} = 0, \qquad A_{30} = 0. \tag{4.28}$$

Boundary conditions (4.6) with (4.8) and the continuity requirements for Z and M_1 result in

$$\begin{aligned}
&A_{20}s^2 + A_{40} + \frac{Ps^4}{64D} = 0,\\
&A_{11}s^2 \ln s + A_{21}s^2 + A_{31} \ln s + A_{41} + \frac{Ps^4}{64D} = 0,\\
&-2sA_{20} + A_{11}s(1 + 2\ln s) + 2A_{21}s - \frac{A_{31}}{s} = 0,\\
&-2A_{20} + A_{11}(3 + 2\ln s) + 2A_{21} - \frac{A_{31}}{s^2} = 0,\\
&A_{11}R^2 \ln R + A_{21}R^2 + A_{31} \ln R + A_{41} + \frac{PR^4}{64D} = 0,\\
&A_{11}[2(1+\nu)\ln R + 3 + \nu] + 2(1+\nu)A_{21} -\\
&-\frac{A_{31}(1-\nu)}{R^2} + \frac{PR^2(3+\nu)}{16D} = 0.
\end{aligned} \tag{4.29}$$

The system (4.29) can be easily solved with respect to unknowns A_{20}, A_{40}, A_{11}, A_{21},

A_{31}, A_{41} and presented as

$$
\begin{aligned}
A_{20} &= \frac{p}{K}\cdot\big[R^6[2(\nu+5)(\ln s-\ln R)+3\nu+13]+\\
&+s^2R^4[4(\nu+3)(\ln s-\ln R)-3\nu-13]+\\
&+s^4R^2[2(\nu+1)(\ln s-\ln R)+\nu-1]+s^6(1-\nu)\big],\\
A_{40} &= \frac{-ps^2R^2}{K}\cdot\big[R^4[2(\nu+5)(\ln s-\ln R)+3\nu+13]+\\
&+4s^2R^2[(\nu+3)(\ln s-\ln R)-\nu-4]+\\
&+s^4[-2(\nu+1)(\ln s-\ln R)+\nu+3]\big],\\
A_{11} &= \frac{2pR^2}{K}\cdot\big[(\nu+5)R^4-2(\nu+3)s^2R^2+(\nu+1)s^4\big],\\
A_{21} &= \frac{-p}{K}\big[R^6[2(\nu+5)\ln R-\nu-3]+\\
&+s^2R^4[4(\nu+3)(\ln R-2\ln s)-\nu+1]+\\
&+s^4R^2[2(\nu+1)\ln R+\nu+3]+s^6(\nu-1)\big],\\
A_{31} &= s^2\cdot A_{11},\\
A_{41} &= \frac{-ps^2R^2}{K}\big[R^4[2(\nu+5)(2\ln s-\ln R)+\nu+3]-\\
&-4s^2R^2[(\nu+3)\ln R+1]+ +s^4[2(\nu+1)\ln R-\nu+1]\big],
\end{aligned}
\tag{4.30}
$$

where $K=64D\big[(\nu-1)s^4-(\nu+3)R^4+4s^2R^2[(\nu+1)(\ln R-\ln s)+1]\big]$.

4.5 Solution of the adjoint system

The adjoint system (4.16) can be integrated after the substitution of (4.25) in (4.16). For the sake of simplicity let us consider the case when $k=1$ in greater detail.

It is easy to recheck that the general solution of (4.16) corresponding to the case

$k = 1$ can be presented as

$$\begin{aligned}
&\psi_1 = \frac{r^2}{2} + C_{1j},\\
&\psi_2 = C_{2j} r + \frac{C_{3j}}{r} - \frac{(3+\nu) r^3}{16} - \frac{C_{1j}(1+\nu) r \ln r}{2},\\
&\psi_3 = \frac{C_{2j} r^2}{D(\nu+1)} + \frac{C_{3j}}{D(\nu-1)} - \frac{r^4}{16D} -\\
&-\frac{C_{1j} r^2}{D(\nu^2-1)} + \frac{C_{1j} r^2 [(1-\nu)\ln r + 1]}{2D(\nu-1)},\\
&\psi_4 = -\frac{C_{2j} r^3}{2D(\nu+1)} - \frac{C_{3j} r \ln r}{D(\nu-1)} + C_{4j} r +\\
&+\frac{r^5}{64D} + \frac{C_{1j} r^3 \ln r}{4D} + \frac{C_{1j}(3 - 2\nu - \nu^2) r^3}{8D(\nu^2-1)}
\end{aligned} \tag{4.31}$$

for $r \in [r_j, r_{j+1}]$ where $j = 0, 1$.

For determination of 8 unknown constants $C_{1j}, C_{2j}, C_{3j}, C_{4j}$ where $j = 0, 1$ one has 8 boundary and intermediate conditions presented by (4.17), (4.18), (4.21) and (4.22).

It immediately follows from boundary conditions (4.17) that

$$C_{10} = 0, \qquad C_{30} = 0. \tag{4.32}$$

The boundary and intermediate conditions (4.18), (4.21), (4.22) lead to the linear

algebraic system

$$
\begin{aligned}
&C_{21}R+\frac{C_{31}}{R}-\frac{C_{11}(1-\nu)R\ln R}{2}-\frac{(3-\nu)R^3}{16}=0,\\
&-\frac{C_{21}R^3(\nu-1)}{2}-C_{31}(\nu+1)R\ln R+C_{41}(\nu^2-1)RD+\\
&+\frac{R^5(\nu^2-1)}{64}+\frac{C_{11}(\nu^2-1)R^3\ln R}{4}+\frac{C_{11}(3-2\nu-\nu^2)R^3}{8}=0,\\
&-\frac{C_{21}s^3(\nu-1)}{2}-C_{31}(\nu+1)s\ln s+C_{41}(\nu^2-1)sD+\\
&+\frac{s^5(\nu^2-1)}{64}+\frac{C_{11}(\nu^2-1)s^3\ln s}{4}+\frac{C_{11}(3-2\nu-\nu^2)s^3}{8}=0,\\
&-\frac{C_{20}s^3(\nu-1)}{2}+C_{40}s(\nu^2-1)D+\frac{s^5(\nu^2-1)}{64}=0,\\
&(C_{21}-C_{20})s+\frac{C_{31}}{s}-\frac{C_{11}(1+\nu)s\ln s}{2}=0,\\
&(C_{21}-C_{20})(\nu-1)s^2+C_{31}(\nu+1)-C_{11}s^2+\\
&+\frac{C_{11}s^2(\nu+1)[(1-\nu)\ln s+1]}{2}=0.
\end{aligned}
\tag{4.33}
$$

From (4.33) one can easily determine the unknown constants C_{20}, C_{40}, C_{11}, C_{21}, C_{31}, C_{41} and presented as

$$
\begin{aligned}
C_{20}&=C_{21}+\frac{C_{31}}{s^2}-\frac{C_{11}(1+\nu)\ln s}{2},\\
C_{40}&=\frac{C_{20}s^2}{2D(\nu+1)}-\frac{s^4}{64D},\\
C_{11}&=\frac{R^2(R^2-s^2)[2R^2(3+\nu)-(\nu+1)(R^2+s^2)]}{8L},\\
C_{21}&=\frac{C_{11}s^2(\nu-1)}{4R^2}+\frac{(3+\nu)R^2}{16}+\frac{C_{11}(1+\nu)\ln R}{2},\\
C_{31}&=\frac{-C_{11}s^2(\nu-1)}{4},\\
C_{41}&=\frac{C_{21}s^2}{2D(\nu+1)}+\frac{C_{31}\ln s}{D(\nu-1)}-\frac{s^4+16C_{11}s^2\ln s}{64D}-\\
&-\frac{C_{11}(-\nu^2-2\nu+3)s^2}{8D(\nu^2-1)},
\end{aligned}
\tag{4.34}
$$

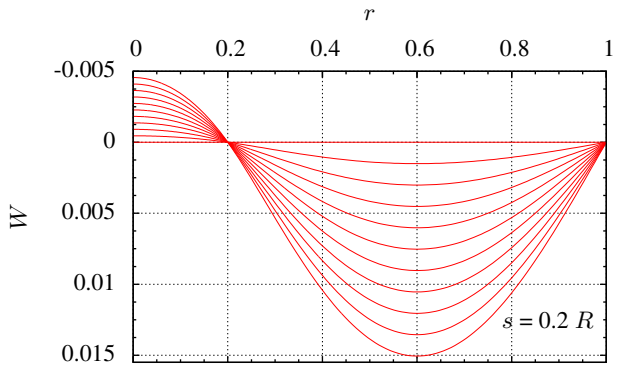

Figure 4.2: Deflection.

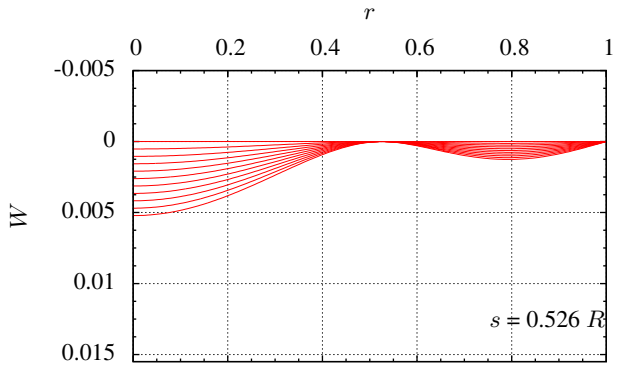

Figure 4.3: Deflection.

where

$$L = s^2(\nu-1)(s^2-R^2) + 2R^2(\nu+1)(s^2-R^2)\ln R - 2R^2s^2(\nu+1)(\ln s - \ln R) +$$

$$+2R^2(\nu+1)(R^2\ln R - s^2\ln s) - R^2(\nu+3)(R^2-s^2).$$

4.6 Discussion of results

Results of calculations are presented in Fig. 4.2 – 4.8. The calculations are implemented for $k = 1$ and $\mu = 0$ in (4.23).

In Fig. 4.2 – 4.4 the distributions of deflections of the plate are presented for various values of the transverse load intensity. Fig. 4.2 and Fig. 4.4 correspond to the

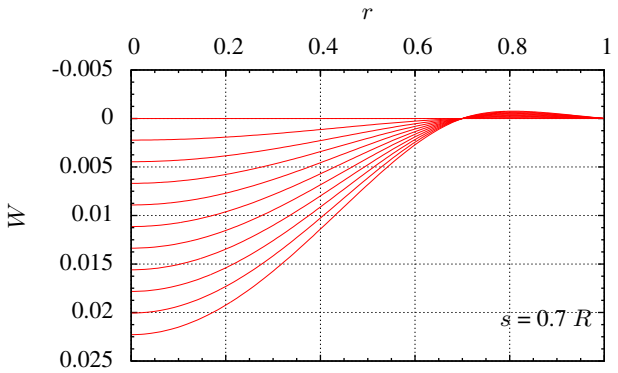

Figure 4.4: Deflection.

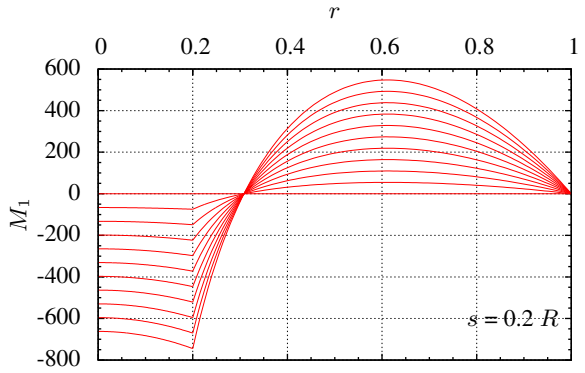

Figure 4.5: Moment.

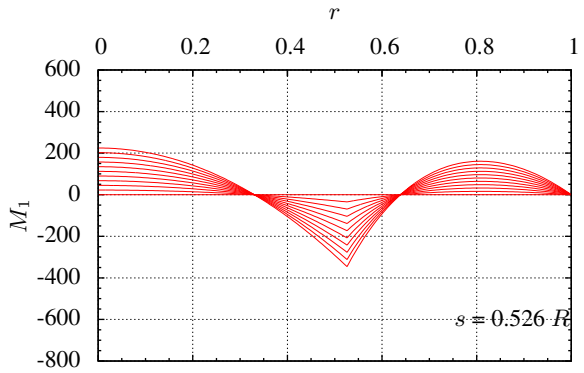

Figure 4.6: Moment.

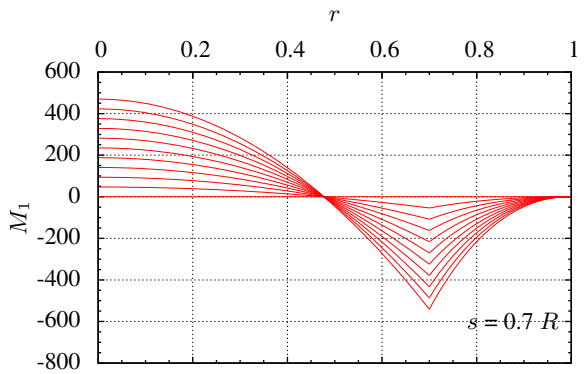

Figure 4.7: Moment.

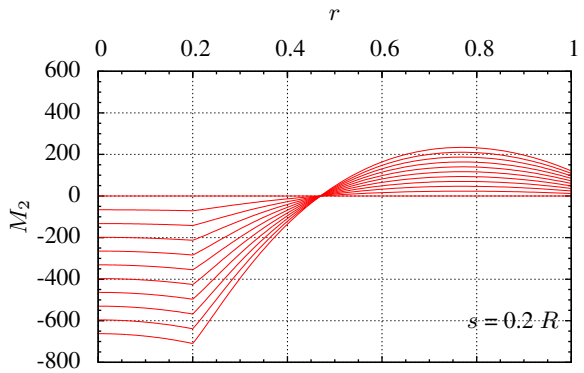

Figure 4.8: Moment.

positions of the support at $s = 0.2R$ and $s = 0.7R$ whereas Fig. 4.3 is associated with the optimal location of the intermediate support. The optimal solution corresponds to $s = 0.526R$. It can be seen from Fig. 4.2 that in the case of smaller values of the radius of the intermediate support deflections at the central part of the plate for $r < 0.2R$ are directed upward despite the pressure is directed downward. Similarily in the case when $s = 0.7R$ one can see negative deflections in the outward region for $r > 0.7R$ (Fig. 4.4). However, in the case of optimal position of the additional support the deflections are non-negative everywhere (Fig. 4.3). It is somewhat surprising that the maximal deflections in the central and outward regions of the plate, respectively, are quite different in the optimal case. However, one has to take into account that the cost function (4.3) with $\mu_0 = 0$, $k = 1$ corresponds to the volume of the axisymmetric body.

In Fig. 4.5 – 4.7 are presented bending moments M_1 for the cases when $s = 0.2R$, $s = 0.7R$ and for the optimal case. It can be seen from Fig. 4.5 – 4.7 that the slope of the radial bending moment has finite jumps at the support position, as might be expected. It is some what surprising that the radial bending moment vanishes at an internal point for any values of the transverse pressure loading. It reveals from Fig. 4.5 that in the case of smaller values of the radius of the internal support the radial bending moment remains negative in the central part of the plate. It is negative in the vicinity of the support in the optimal case, as well.

Distributions of the circumferential bending moment M_2 are presented in Fig. 4.8 for different values of the pressure loading. Here $s = 0.2R$. It reveals from Fig. 4.8 that the bending moment M_2 is unexpectedly continuous at $r = s$.

CHAPTER 5
ANISOTROPIC PLATE

5.1 Formulation of the problem

Let us consider a circular plate of radius R made of a undirectionally reinforced composite material. It is assumed that the fibers are embedded in the matrix material more or less uniformly with enough high density so that the material can be modelled as a quasi homogeneous anisotropic material. In the present paper two cases of undirectional reinforcement will be considered. These are the radial and the circumferential reinforcements, respectively.

The plate under cosideration is simply supported at the edge and it is subjected to the axisymmetric tranverse pressure loading of intensity $P(r)$ where r stands for the current radius. Under these assumptions it is reasonable to presume that the stress strain state of the plate remains axisymmetric during the deformation.

The thickness h of the plate is assumed to be piecewise constant, e.g. $h = h_j$ for $r \in (a_j, a_{j+1})$ where $j = 0, \ldots, n$. Note that in the case of a sandwich plate the quantity h is interpreted as the thickness of carrying layers.

The parameters h_j, a_j are treated as preliminarily unknown parameters to be determined so that maximal deflection $W_0 = W(0)$ attains the minimal value under given weight or material volume of the plate. The latter can be presented as

$$V = \pi \sum_{j=0}^{n} h_j (a_{j+1}^2 - a_j^2). \tag{5.1}$$

It is stipulated in (5.1) that $a_0 = 0$, $a_{n+1} = R$.

5.2 Equations of equilibrium and strain components

In the present paper the governing equations of the classical bending theory of thin plates will be used. It can be shown that an element of the plate is in equilibrium if the following equations are satisfied (see Reddy [**?**], Kaliszky [**?**], Ventsel and Krauthammer [**?**])

$$\begin{aligned} &\frac{d}{dr}(rM_1) - M_2 - rQ = 0, \\ &\frac{d}{dr}(rQ) + P(r) \cdot r = 0. \end{aligned} \tag{5.2}$$

Here M_1 and M_2 stand for the bending moments in the radial and circumferential direction, respectively, and Q is the shear force. The stress strain state of the plate is

assumed to be axisymmetric, e.g. the state is identical for each Θ, Θ being the polar angle and r current radius. The membrane forces meet the equation

$$\frac{d}{dr}(rN_1) - N_2 = 0 \tag{5.3}$$

where the subscripts indicate the same directions as in the previous formula.

The generalized stresses are coupled with the principal stresses as

$$\begin{aligned} N_{1,2} &= \int_{-\frac{h}{2}}^{\frac{h}{2}} \sigma_{1,2} dz \\ M_{1,2} &= \int_{-\frac{h}{2}}^{\frac{h}{2}} \sigma_{1,2} z dz \end{aligned} \tag{5.4}$$

where σ_1, σ_2 stand for the normal stresses in the radial and circumferential direction, respectively. Here h and z are the thickness and the coordinate in the transversal direction, respectively.

The principle of virtual work states that

$$\delta E_i = \delta A_e. \tag{5.5}$$

Here δE_i stands for the variation of the internal energy induced by virtual displacements. In the case of axisymmetric plates (see Jones [**?**], Ventsel and Krauthammer [**?**])

$$\delta E_i = \int_a^R (M_1 \delta \varkappa_1 + M_2 \delta \varkappa_2) r dr \tag{5.6}$$

whereas (here $P(r)$ is the tranverse pressure and W the deflection)

$$\delta A_e = \int_a^R P(r) \delta W r dr \tag{5.7}$$

where $\varkappa_1$ and $\varkappa_2$ stand for the principal curvatures. It is well known that in the case of circular and annular plates (see Jones [**?**], Reddy [**?**], Vinson [**?**])

$$\begin{aligned} \varkappa_1 &= -\frac{d^2 W}{dr^2}, \\ \varkappa_2 &= -\frac{1}{r}\frac{dW}{dr}. \end{aligned} \tag{5.8}$$

Note that the principle of virtual work in the form (5.5)-(5.8) holds good in the case of axisymmetric deformations under the condition that shear deformations as well as the in-plane displacements can be disregarded. The in-plane displacements are taken into account in the non-linear plate theories.

5.3 Constitutive equations

It is known that in a unidirectional fiber-reinforced layer of material two perpendicular planes of symmetry exist at each point. The intersections of these planes with the middle plane of the lamina define two directions denoted by subscripts 1 and 2, respectively. These directions called principal axis of orthotropy correspond to the direction of fibers and a direction transverse to the fibers.

In an orthotropic layer the assumptions of the plane stress hold good and thus the Hooke's law reads (see Daniel and Ishai [**?**], Jones [**?**])

$$\left\{ \begin{array}{c} \sigma_1 \\ \sigma_2 \\ \tau_{12} \end{array} \right\} = [Q] \cdot \left\{ \begin{array}{c} \varepsilon_1 \\ \varepsilon_2 \\ \gamma_{12} \end{array} \right\} \tag{5.9}$$

where σ_1, σ_2, τ_{12} are the stress components and ε_1, ε_2, γ_{12} corresponding strain components. The matrix $[Q]$ is defined as

$$[Q] = \left[\begin{array}{ccc} Q_{11} & Q_{12} & 0 \\ Q_{12} & Q_{22} & 0 \\ 0 & 0 & Q_{66} \end{array} \right]. \tag{5.10}$$

The elements Q_{ij} in (5.10) are so-called reduced stiffnesses related to the material constants. Let us denote by E_1, E_2 Young's moduli in two principal directions and by ν_{12}, ν_{21} corresponding Poisson's ratios.

For any combination of fibers and the matrix

$$\frac{\nu_{12}}{E_1} = \frac{\nu_{21}}{E_2} \tag{5.11}$$

and the reduced stiffnesses are

$$\begin{aligned} Q_{11} &= \frac{E_1}{1 - \nu_{12}\nu_{21}}, \quad Q_{22} = \frac{E_2}{1 - \nu_{12}\nu_{21}} \\ Q_{12} &= \frac{\nu_{21} E_1}{1 - \nu_{12}\nu_{21}}, \quad Q_{66} = G_{12}. \end{aligned} \tag{5.12}$$

It can be seen from (5.11), (5.12) that in the constitutive relations (5.9), (5.10) can be presented via four independent material constants.

In the following the main attention will be focused at the determination of bending moments assuming that the contribution of membrane forces and in-plane displacements to the stress strain state is relatively small in the range of small displacements. Thus, assuming that the fibers are embedded in the matrix material in the radial or circumferential direction only and that

$$\begin{aligned} \varepsilon_1 &= z\varkappa_1, \\ \varepsilon_2 &= z\varkappa_2 \end{aligned} \tag{5.13}$$

it follows from (5.9)

$$\begin{aligned} \sigma_1 &= z(Q_{11}\varkappa_1 + Q_{12}\varkappa_2), \\ \sigma_2 &= z(Q_{12}\varkappa_1 + Q_{22}\varkappa_2). \end{aligned} \tag{5.14}$$

Substituting (5.14) in (5.4) and taking (5.11), (5.12) into account one obtains

$$\begin{aligned} M_1 &= DE_1(\varkappa_1 + \nu_{21}\varkappa_2), \\ M_2 &= DE_2(\nu_{12}\varkappa_1 + \varkappa_2) \end{aligned} \tag{5.15}$$

where

$$D = \frac{h^3}{12(1-\nu_{12}\nu_{21})}. \tag{5.16}$$

For regions of constant thickness where $h = h_j = const$ it is reasonable to denote

$$D_j = \frac{h_j^3}{12(1-\nu_{12}\nu_{21})}. \tag{5.17}$$

Equations (5.15) with (5.16) present the constitutive equations for anisotropic (in the present case for orthotropic) layers and plates. Substituting the curvatures $\varkappa_1$, $\varkappa_2$ by the help of (5.8) in (5.15) one obtains

$$\begin{aligned} M_1 &= -E_1 D_j \left(\frac{d^2W}{dr^2} + \frac{\nu_{21}}{r}\frac{dW}{dr} \right), \\ M_2 &= -E_2 D_j \left(\frac{\nu_{12}d^2W}{dr^2} + \frac{1}{r}\frac{dW}{dr} \right) \end{aligned} \tag{5.18}$$

for $r \in (a_j, a_{j+1})$, where $j = 0, \ldots, n$.

5.4 Solution of governing equations

Let us consider the case when the intensity of the transverse loading $P(r) = P = const$ in a greater detail. In this case the second equation in the system (5.2) can be easily integrated. In fact, the differentiation of the first equation in (5.2) and the substitution of the shear force results in

$$\frac{d}{dr}\left[\frac{d}{dr}(rM_1) - M_2\right] = -Pr. \tag{5.19}$$

The integration of (5.19) gives

$$\frac{d}{dr}(rM_1) - M_2 = -\frac{Pr^2}{2} - B_{0j} \tag{5.20}$$

for $r \in (a_j, a_{j+1})$, $j = 0, \ldots, n$. Here B_{0j} stands for an arbitrary constant.

Substituting the bending moments from (5.18) in (5.20) and accounting for the relation (5.11) results in

$$\frac{rd^3W}{dr^3} + \frac{d^2W}{dr^2} - \frac{E_2}{E_1} \cdot \frac{1}{r}\frac{dW}{dr} = \frac{Pr^2}{2E_1D_j} + \frac{B_{0j}}{E_1D_j} \tag{5.21}$$

for $r \in (a_j, a_{j+1})$. The shear force Q must be continuous at each $r \in [a, R]$. Thus $Q(a_j - 0) = Q(a_j + 0)$. Therefore, one can write

$$B_{0j} = B_0 \tag{5.22}$$

for each $j = 0, \ldots, n$. Indeed, it immediately follows from (5.2), (5.20) that

$$Q(r) = \frac{1}{r}\left(-\frac{Pr^2}{2} - B_{0j}\right) \tag{5.23}$$

for $r \in (a_j, a_{j+1})$, $j = 0, \ldots n$. Thus at $r = a_j \pm 0$ one has

$$-\frac{Pa_j}{2} - \frac{B_{0j-1}}{a_j} = -\frac{Pa_j}{2} - \frac{B_{0j}}{a_j}. \tag{5.24}$$

From (5.24) one can see that $B_{0j-1} = B_{0j}$ for each $j = 1, \ldots, n$ and therefore, (5.22) holds good.

Let us concentrate on the integration of the equation (5.21). It is reasonable to denote

$$E_2 = k^2 E_1. \tag{5.25}$$

Multiplying the both sides of (5.21) to r and integrating results in the second order diffrential equation (here C_{0j} is an arbitrary constant)

$$\begin{aligned} &\frac{r^2d^2W}{dr^2} - \frac{rdW}{dr} + (1-k^2)W = \\ &= \frac{Pr^4}{8E_1D_j} + \frac{B_0r^2}{2E_1D_j} + C_{0j}(1-k^2) \end{aligned} \tag{5.26}$$

for $r \in (a_j, a_{j+1})$. This is a linear non-homogeneous equation. The general solution of (5.26) consists of the sum of the general solution of corresponding homogeneous equation

$$W_h = C_{1j}r^{1+k} + C_{2j}r^{1-k} \tag{5.27}$$

and of a particular solution of (5.26). The latter can be presented as

$$\begin{aligned} W_p = &\frac{Pr^4}{8(9-k^2)E_1D_j} + \\ &+ \frac{B_0r^2}{2(1-k^2)E_1D_j} + C_{0j}. \end{aligned} \tag{5.28}$$

In (5.27), (5.28) C_{0j}, C_{1j} and C_{2j} are arbitrary constants of integration.

Finally, the general solution of (5.26) for $(r \in a_j, a_{j+1})$, $j = 0, \ldots, n$ can be presented as

$$\begin{aligned} W &= C_{0j} + C_{1j} r^{1+k} + C_{2j} r^{1-k} + \\ &+ \frac{P r^4}{8(9-k^2) E_1 D_j} + \frac{B_0 r^2}{2(1-k^2) E_1 D_j}. \end{aligned} \tag{5.29}$$

From (5.29) one easily obtains

$$\begin{aligned} \frac{dW}{dr} &= C_{1j}(1+k) r^k + C_{2j}(1-k) r^{-k} + \\ &+ \frac{P r^3}{2(9-k^2) E_1 D_j} + \frac{B_0 r}{(1-k^2) E_1 D_j}, \\ \frac{d^2 W}{dr^2} &= C_{1j} k (1+k) r^{k-1} + \\ &+ C_{2j}(1-k)(-k) r^{-k-1} + \\ &+ \frac{3 P r^2}{2(9-k^2) E_1 D_j} + \frac{B_0}{(1-k^2) E_1 D_j}. \end{aligned} \tag{5.30}$$

Substitution of (5.30) in (5.18) results in

$$\begin{aligned} M_1 &= -E_1 D_j \Big[C_{1j}(1+k)(k+\nu_{21}) r^{k-1} + \\ &+ C_{2j}(1-k)(\nu_{21}-k) r^{-k-1} + \\ &+ \frac{P r^2 (3+\nu_{21})}{2 E_1 D_j (9-k^2)} + \frac{B_0 (1+\nu_{21})}{E_1 D_j (1-k^2)} \Big], \\ M_2 &= -E_2 D_j \left[C_{1j}(1+k)(k\nu_{12}+1) \cdot \right. \\ &\cdot r^{k-1} + C_{2j}(1-k)(1-k\nu_{12}) r^{-k-1} + \\ &+ \left. \frac{P r^2 (1+3\nu_{12})}{2 E_1 D_j (9-k^2)} + \frac{B_0 (1+\nu_{12})}{E_1 D_j (1-k^2)} \right] \end{aligned} \tag{5.31}$$

which hold good for $r \in (a_j, a_{j+1})$, $j = 0, \ldots, n$.

The governing equations (5.2) are accompanied with boundary conditions

$$M_1(R) = 0, \qquad W(R) = 0 \tag{5.32}$$

and

$$\frac{dW(0)}{dr} = 0 \tag{5.33}$$

in the case of a simply supported plate. If membrane forces are taken into account extra requirements for in-plane quantities are needed.

5.5 Bending of a one-stepped plate

Let us focuse our attention to the plate of piecewise constant thickness

$$h = \begin{cases} h_0; r \in (0, a) \\ h_1; r \in (a, R). \end{cases} \tag{5.34}$$

For determination of the stress strain state of the plate one can use the relations (5.29) – (5.33) for $n = 1$ and corresponding continuity requirements for the deflection W and the bending moment M_1.

From physical considerations it is evident that the quantities W, $\frac{dW}{dr}$, M_1 and M_2 must be finite at the center of the plate (for $r = 0$). This is possible only in the case where (here $k > 0$)

$$C_{10} = 0, \qquad C_{20} = 0. \tag{5.35}$$

Bearing (5.35) in mind one can simplify the notation equalizing

$$C_{00} = W_0,\ C_{01} = C,\ C_{11} = C_1,\ C_{21} = C_2. \tag{5.36}$$

The continuity of the radial bending moment at $r = a$ leads to the relation

$$\begin{aligned} &C_1(1+k)(k+\nu_{21})a^{k-1}+ \\ &+C_2(1-k)(\nu_{21}-k)a^{-k-1} = 0. \end{aligned} \tag{5.37}$$

It is easy to deduce from (5.37)

$$C_2 = -\frac{C_1(1+k)(k+\nu_{21})a^{2k}}{(1-k)(\nu_{21}-k)}. \tag{5.38}$$

Employing the continuity condition for $\frac{dW}{dr}$ to (5.30), (5.33) one has

$$\begin{aligned} &C_1(1+k)a^k + C_2(1-k)a^{-k}+ \\ &+\frac{Pa^3}{2(9-k^2)E_1D_1} + \frac{B_0 a}{(1-k^2)E_1D_1} = \\ &= \frac{Pa^3}{2(9-k^2)E_1D_0} + \frac{B_0 a}{(1-k^2)E_1D_0}. \end{aligned} \tag{5.39}$$

From (5.39) one can easily determine

$$B_0 = (1-k^2)E_1D_1\cdot$$
$$\cdot\left[\frac{2k(1+k)D_0a^{k-1}C_1}{(k-\nu_{21})(D_1-D_0)}-\right. \tag{5.40}$$
$$\left.-\frac{Pa^2}{2E_1D_1(9-k^2)}\right].$$

The first requirement in (5.32) with (5.31), (5.38) and (5.40) admits to define

$$C_1 = \frac{(k-\nu_{21})(\gamma-1)PR^2}{2(9-k^2)(1+k)E_1D_1R^{k-1}}\cdot$$
$$\cdot\frac{\alpha^2(1+\nu_{21})-3-\nu_{21}}{N},$$
$$C_2 = \frac{(k+\nu_{21})PR^2\alpha^{2k}(\gamma-1)}{2(9-k^2)E_1D_1R^{-k-1}}\cdot \tag{5.41}$$
$$\cdot\frac{\alpha^2(1+\nu_{21})-3-\nu_{21}}{N}$$

where for the conciseness sake the notation

$$N = (k^2-\nu_{21}^2)(1-\alpha^{2k})(\gamma-1)+$$
$$+2k(1+\nu_{21})\alpha^{k-1} \tag{5.42}$$

and

$$\gamma = \frac{D_1}{D_0}, \qquad \alpha = \frac{a}{R} \tag{5.43}$$

is introduced.

According to the second boundary condition in (5.32) and (5.29) one has

$$C + C_1R^{k+1} + C_2R^{1-k}+$$
$$+\frac{PR^4}{8(9-k^2)E_1D_1} + \frac{B_0R^2}{2(1-k^2)E_1D_1} = 0. \tag{5.44}$$

The last equation with (5.38), (5.40), (5.43) admits to define

$$C = \frac{PR^4(2\alpha^2-1)}{8(9-k^2)E_1D_1} + R^{k+1}C_1\cdot$$
$$\cdot\left[\frac{(1+k)(k+\nu_{21})\alpha^{2k}}{(1-k)(\nu_{21}-k)} -\right. \tag{5.45}$$
$$\left.-\frac{k(1+k)}{(k-\nu_{21})(\gamma-1)}-1\right].$$

Employing the continuity of the deflection W at $r = a$ one obtains

$$W_0 + \frac{Pa^4}{8(9-k^2)E_1D_0} + \\ + \frac{B_0a^2}{2(1-k^2)E_1D_0} = \frac{Pa^4}{8(9-k^2)E_1D_1} + \\ + \frac{B_0a^2}{2(1-k^2)E_1D_1} + C_1a^{1+k} + C_2a^{1-k}. \tag{5.46}$$

Thus the maximal deflection can be calculated as

$$W_0 = \left[\frac{Pa^4}{8(9-k^2)} + \frac{B_0a^2}{2(1-k^2)}\right] \cdot \\ \cdot \frac{1-\gamma}{E_1D_1} + C_1a^{k+1} + C_2a^{1-k} \tag{5.47}$$

where the constants B_0, C_1 and C_2 are defined by (5.40), (5.41), (5.43).

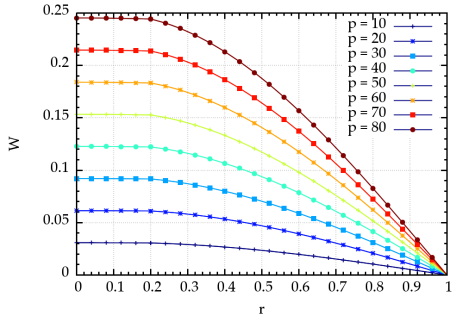

Figure 5.1: Deflections of the plate.

5.6 Optimal design of a stepped plate

The problem posed above consists in the minimization of the maximal deflection $W_0 = W(0)$ under the condition that the material volume of the plate is constrained.

Evidently, the deflection $W(0)$ is a function of design parameters; $W_0 = W_0(a_1, \ldots, a_n, h_0, \ldots, h_n)$. The constrained minimum of W_0 can be defined employing the extended function

$$I_* = W_0(a_1, \ldots, a_n, h_0, \ldots, h_n) + \lambda(V - V_0) \tag{5.48}$$

where λ is an unknown Lagrangeian multiplier.

The necessary optimality conditions of (5.48) can be written as

$$\begin{aligned} &\frac{\partial I_*}{\partial a_i} = 0; \qquad i = 1, \ldots, n \\ &\frac{\partial I_*}{\partial h_j} = 0; \qquad j = 0, \ldots, n \\ &\frac{\partial I_*}{\partial \lambda} = 0. \end{aligned} \tag{5.49}$$

The system (5.49) consists of $2n + 2$ algebraic equations. These admit to determine $2n+2$ unknown parameters a_i $(i = 1, \ldots, n)$, h_j $(j = 0, \ldots, n)$ and λ for each given volume of the plate V_0.

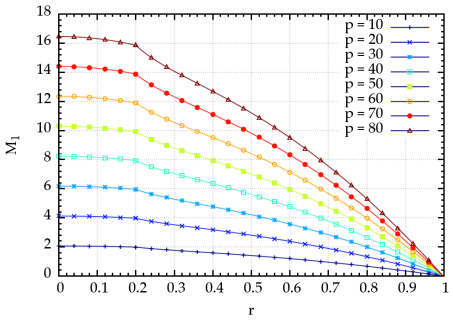

Figure 5.2: Radial bending moments.

5.7 Numerical results and discussion

The non-linear system of equations (5.49) is solved numerically. Calculations are carried out with the aid of computer codes Python and Mathematica.

The results of calculations are presented in the Table 1 and Fig. 1–3 for the case $n = 1$. The results are obtained for the plate made of a Boron-Aluminium composite consisting of Aluminium matrix and Boron fibers. For this material $E_1 = 204$ GPa, $E_2 = 118$ GPa and $\nu_{12} = 0.27$.

The displacements in the transverse direction are presented for different values of the intensity of the transverse pressure in Fig. 1. The radial and circumferential bending moments are depicted in Fig. 2 and Fig. 3, respectively, for different load levels for the stepped plate with the step at $a = 0.2R$.

It can be seen from Fig. 3 that the circumferential bending moment is discontinuous at $r = a$, as might be expected. Calculations carried out showed that the jump of M_2 at $r = a$ depends on the ratio of thicknesses in the adjacent sections of the plate.

Table 5.1: Optimal values of parameters.

V_0	W_o	α	γ	W_*	e
0.45	0.0056	0.5701	0.1852	0.0262	0.2122
0.50	0.0044	0.5475	0.2860	0.0191	0.2306
0.55	0.0039	0.5466	0.3583	0.0143	0.2685
0.60	0.0035	0.5539	0.4230	0.0111	0.3146
0.65	0.0032	0.5670	0.4842	0.0087	0.3678
0.70	0.0030	0.5852	0.5437	0.0070	0.4278
0.75	0.0028	0.6088	0.6028	0.0057	0.4952
0.80	0.0027	0.6384	0.6624	0.0047	0.5709
0.85	0.0026	0.6755	0.7241	0.0039	0.6561
0.90	0.0025	0.7232	0.7904	0.0033	0.7530
0.95	0.0024	0.7887	0.8677	0.0028	0.8651
0.99	0.0024	0.8659	0.9600	0.0025	0.9705

The radial bending moment M_1 has slope discontinuity at the step position (Fig. 2) which is less remarkable in the cases of lower load intensities.

The efficiency of the design established above is assessed by the ratio

$$e = \frac{W_0}{W_*}, \tag{5.50}$$

W_* being the deflection of the plate of constant thickness $h_* = V_0 h_0$. The values of the coefficient e are accommodated in Table 1 together with optimal values α and γ. In the first column of Table 1 the values of the plate volume $V_0 = \frac{V}{\pi}$ are presented. It reveals form Table 1 that for smaller values of V_0 the deflection of the reference plate of constant thickness W_* is larger, as might be expected. If V_0 increases then the optimal ratio of thicknesses $\gamma = \frac{h_1}{h_0}$ also increases and the step location $a = \alpha R$ moves towards the edge of the plate. However, the maximal deflection of the optimized plate decreases if the quantity V_0 increases.

Calculations carried out showed that the optimal values of α and γ are insensitive with respect to the changes of the load intensity. However, the optimal value of W_0 as well as the quantities W_* and e do depend on the value of the load intensity P.

5.8 Conclusions

A method for analysis and optimization of fiber reinforced composite plate was developed. Considering the cases of unidirectional orientations of fibers the composite was modelled as a quasi homogeneous anisotropic material having different proper-

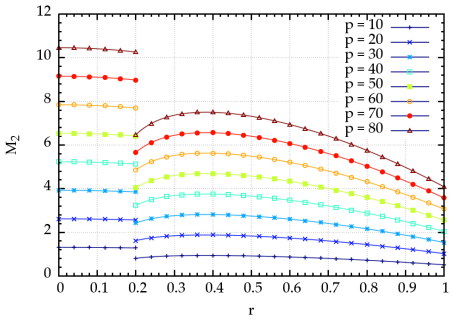

Figure 5.3: Circumferential bending moments.

ties in different directions. In the paper the attention was focused on the cases of radial and circumferential orientation of fibers in the matrix material.

Invoking the methods of non-linear mathematical programming the optimal design parameters of plates with piecewise constant thickness are determined. The optimization problems are solved with the aid unknown Lagrangeian multipliers. Numerical results are obtained with the aid of existing computer codes. It was shown that the optimal values of design parameters depend on the physical and geometrical parameters but these are insensitive with respect to the loading level.

ACKNOWLEDGEMENTS

I am deeply grateful to my supervisors Enn Saar and Peeter Tenjes for their patient supervision and teaching. They both have helped me to overcome many obstacles on the bumpy road of becoming an astrophysicist. I am also very thankful for their advice on improving my manuscript.

I feel specially indebted to my senior colleague at the Tartu Observatory, Jaan Einasto, for the fruitful discussions and conversations, which helped to start the study that finally formed the present thesis.

My sincere gratitude goes to my colleagues at the Tartu Observatory Antti Tamm, Lauri Juhan Liivamägi, Maret Einasto, Mirt Gramann, Erik Tago, and Taavi Tuvikene for the fruitful collaboration and their contribution to the studies.

I am also thankful to my colleague Jaan Pelt who offered several time a personal assistance and advice for specific mathematical and statistical problems.

I would like to thank Volker Müller for his support and hospitality during my stays at the Astrophysikalisches Institut Potsdam. This visits provided vital support to my research and allowed to finalise my thesis.

Carrying out this study has become possible due to the existence of the SDSS and 2dFGRS surveys and I express my gratitude to all the people involved.

I gratefully acknowledge the financial support by the Estonian Science Foundation and the Estonian Ministry of Education.

REFERENCES

[1] B. Akesson and N. Olhoff. Minimum stiffness of optimally located supports for maximum value of beam eigenfrequences. *J. Sound Vibr.*, 120:457–463, 1988.

[2] H. G. Allen. *Analysis and Design of Structural Sandwich Panels*. Pergamon Press, Oxford, 1969.

[3] N. Banichuk. *Introduction to Optimization of Structures*. Springer, Berlin, 1990.

[4] D. Bojczuk and Z. Mroz. On optimal design of supports in beam and frame structures. *Struct. Optimiz.*, 16,1:47–57, 1998.

[5] D. Bojczuk and Z. Mroz. Determination of optimal actuator forces and positions in smart structures using adjoint method. *Struct. Multidisc. Optim.*, 30,4:308–319, 2005.

[6] A. Bryson and H. Yu-Chi. *Applied Optimal Control*. Wiley, New York, 1975.

[7] J. Chakrabarty. *Applied Plasticity*. Springer, Berlin, 2006.

[8] M. Z. Cohn. *Analysis and Design of inelastic Structures*. University of Waterloo Press, Waterloo, 1972.

[9] G. Eason. The elastic, plastic bending of a simply supported plate. *J. Appl. Mech.*, 28,3:395–401, 1961.

[10] F. W. French. Elastic-plastic analysis of centrally clamped annular plates under uniform loads. *Journal of the Franklin Institute*, 277,6:575–592, 1964.

[11] A. Garstecki and Z. Mroz. Optimal design of supports of elastic structures subjected to loads and initial distortions. *Mech. Struct. Mach.*, 15:47–68, 1987.

[12] D. G. Hull. *Optimal Control Theory for Applications*. Springer, Berlin, 2003.

[13] S. Kaliszky. *Plasticity. Theory and Engineering Applications*. Elsevier, Amsterdam, 1989.

[14] J. Lellep. Optimal location of additional supports for plastic cylindrical shells subjected to impulsive loading. *Int. J. Non-Linear Mech.*, 19,4:323–330, 1984.

[15] J. Lellep. Optimum location of additional supports for a geometrically nonlinear plastic cylindrical shell. *Soviet Applied Mechanics*, 21,1:54–60, 1985.

[16] J. Lellep. Parametrical optimization of plastic cylindrical shells in the post-yield range. *Int. J. Eng. Sci.*, 23,12:1289–1303, 1985.

[17] J. Lellep. Optimal design of plastic reinforced cylindrical shells. *Control-Theory and Advanced Technology*, 5,2:119–135, 1989.

[18] J. Lellep and Ü. Lepik. Analytical methods in plastic structural design. *Eng. Optimization*, 7,3:209–239, 1984.

[19] J. Lellep and A. Paltsepp. Optimization of inelastic cylindrical shells with internal supports. *Struct. Multidisc. Optim.*, pages 841–852, 2010.

[20] J. Lellep and J. Polikarpus. Optimization of elastic-plastic circular plates under axisymmetric loading. *Proc. 20th Intern. Conference "Continuous Optimization and Knowledge-Based Technology"*, pages 291–295, 2008.

[21] J. Lellep and J. Polikarpus. Elastic plastic bending of stepped annular plates. *American Conf. on Applied Mathematics "Applications of Mathematics & Computer Engineering"*, pages 140–145, 2011.

[22] J. Lellep and J. Polikarpus. Optimization of elastic circular plates with additional supports. *2nd Int. Conf. on Theoretical and Applied Mechanics "Recent Researches in Mechanics"*, pages 136–141, 2011.

[23] J. Lellep and E. Puman. Optimization of elastic and inelastic conical shells of piece wise constant thickness. *2nd Int. Conf. on Theoretical and Applied Mechanics "Recent Researches in Mechanics"*, pages 223–228, 2011.

[24] J. Lellep, E. Puman, L. Roots, and E. Tungel. Optimization of rotationally symmetric shells. *14th WSEAS Int. Conf. Applied Mathematics "Recent Advances in Applied Mathematics"*, pages 233–238, 2009.

[25] J. Lellep, E. Puman, L. Roots, and E. Tungel. Optimization of stepped shells. *WSEAS Transactions on Mathematics*, 9,2:130–139, 2010.

[26] Ü. Lepik. Optimal design of beams with minimum compliance. *Int. J. Non-Linear Mech.*, 13,1:33–42, 1978.

[27] Z. Mroz and T. Lekszycki. Optimal support reaction in elastic frame structures. *Computers and Structures*, 14:179–185, 1981.

[28] P. M. Naghdi. Bending of elastoplastic circular plates with large deflection. *Journal of Applied Mechanics*, 19:293–300, 1952.

[29] N. Olhoff and B. Akesson. Minimum stiffness of optimally located supports for minimum value of column buckling loads. *J. Struct. Optim.*, 3:163–175, 1991.

[30] F. J. Plantema. *Sandwich Construction: the Bending and Buckling of Sandwich Beams, Plates and Shells*. Wiley and Sons, New York, 1966.

[31] W. Prager and G. Rozvany. Plastic design of beams: optimal locations of supports and steps in yield moment. *Int. J. Mech. Sci.*, 17,10:627–631, 1975.

[32] J. N. Reddy. *Theory and Analysis of Elastic Plates and Shells*. CRC Press, Boca Raton, 2007.

[33] G. Rozvany. *Structural Design via Optimality Criteria*. Kluwer, Dordrecht, 1989.

[34] M. A. Save, C. E. Massonnet, and G. De Saxce. *Plastic Limit Analysis of Plates, Shells and Disks*. Elsevier, Amsterdam, 1997.

[35] A. Sawczuk and J. Sokól-Supel. *Limit Analysis of Plates*. Polish Scientific Publishers, Warsaw, 1993.

[36] A. N. Sherbourne and N. K. Srivastava. Elastic-plastic bending of restrained pin-ended circular plates. *International Journal of Mechanical Sciences*, 13,3:231–241, 1971.

[37] D. Szelag and Z. Mroz. Optimal design of elastic beams with unspecified support positions. ZAMM, 58:501–510, 1978.

[38] B. Tekinalp. Elastic-plastic bending of a built-in circular plate under a uniformly distributed load. *Journal of Mechanics and Physics of Solids*, 5,2:135–142, 1957.

[39] G. J. Turvey and M. Salehi. Computer generated elasto-plastic design data for pressure loaded circular plates. *Computers and Structures*, 41,6:1329–1340, 1991.

[40] E. Ventsel and T. Krauthammer. *Thin Plates and Shells: Theory, Analysis and Applications*. Marcel Dekker, New York, 2001.

[41] J. Vinson. *Plate and Panel Structures of Isotropic, Composite and Piezoelectric Materials, Including Sandwich Construction*. Springer, Dordrecht, 2005.

[42] C. M. Wang, Y. Xiang, S. Kitiporncha, and K. M. Liew. Axisymmetric buckling of circular Mindlin plate with ring supports. *J. Struct. Eng.*, 119,3:782–793, 1993.

[43] D. Wang. Optimization of support positions to minimize the maximal deflections of structures. *Int. J. Solids Structures*, 41,26:7445–7458, 2004.

[44] T. X. Yu and L. C. Zhang. *Plastic Bending. Theory and Applications*. World Scientific, Singapore, 1996.

SUMMARY IN ESTONIAN

Galaktikate evolutsiooni mõistmine nende heledusfunktsiooni abil

Galaktikad, mis koosnevad kuni sadadest miljarditest tähtedest, gaasist ja tolmust, on ühed tähelepanuväärsemad süsteemid Universumis. Juba visuaalsete vaatluste põhjal on näha, et neid on väga mitmesuguseid: spiraalseid, elliptilisi ning lisaks ka korrapäratu kujuga. Selline mitmekesisus tekitab küsimuse, kuidas galaktikad on tekkinud ning millised füüsikalised protsessid on galaktikate evolutsioonis olulised? Kuna galaktikate tekkimine ja evolutsioon hõlmab paljusid erinevaid füüsikalisi protsesse ning on seetõttu üsna komplitseeritud, siis on galaktikate tekkimine tänapäeva kosmoloogias üks aktuaalsemaid teemasid. Galaktikate evolutsioni parem mõistmine on ka antud uurimuse üks eesmärke.

Praeguse üldtunnustatud arusaama järgi tekivad galaktikad tumeaine halodes, kuhu koondub gaas ning kus peale gaasi piisavat jahtumist algab täheteke. Galaktikate tekkimine ja evolutsioon toimub hierarhilise arenguna: kõigepealt tekivad väiksemad süsteemid ning nende järk-järgulisel liitumisel tekivad üha suuremad süsteemid. Sellise hierarhilise kuhjumise kestel toimub väga palju galaktikate omavahelisi põrkeid ning ühinemisi, mis kõik mõjutavad galaktikate arengut.

Tänapäeva kosmoloogias on küllaltki hästi teada põhilised füüsikalised protsessid, mis mõjutavad galaktikate arengut. Peamiste protsessidena võib välja tuua galaktikate põrgetel toimuvad gravitatsioonilised häiritused, tekkivad lööklained, gaasi ümberpaiknemine, tiheduse muutused, täheteke ja supernoovade plahvatused, aktiivsete galaktikatuumade mõju ning galaktikate liikumine läbi galaktikate vahelise keskkonna. Hoolimata sellest, et me teame olulisemaid galaktikate arengut mõjutavaid protsesse, on galaktikate tekkimine tervikuna tunduvalt halvemini teada. Peamiseks põhjuseks on asjaolu, et me ei tea piisava täpsusega, milliste füüsikaliste tingimuste juures ja milliste keskkonna parameetrite puhul on eelpool nimetatud füüsikalised protsessid olulised. Kasutades pool-analüütilisi mudeleid, on praeguseks siiski küllaltki palju uuritud erinevaid protsesse sõltuvana kujunevate galaktikate lokaalsest ümbrusest. Lokaalse ümbrusena vaadeldakse peamiselt galaktika gruppe ja parvi.

Vaatluslikust kosmoloogiast on teada, et galaktika grupid ja parved ei paikne Universumis juhuslikult, vaid moodustavad suuremastaabilise kärgstruktuuri – superparvede ja tühikute võrgustiku. Kuidas galaktikate areng sõltub suuremastaabilisest struktuurist ning kas tühikutes ja superparvedes tekivad galaktikad sarnaselt või erinevalt, on küllaltki vähe uuritud. Et uurida suuremastaabilise sturktuuri mõju, on vaja kasutada suuri galaktikate valimeid. Kasutades viimastel aastatel valminud suuri galaktikate taevaülevaateid on tekkinud võimalus antud probleemi uurida vaatluslikult. Ühtedeks olulistemaks taevaülevaadeteks on 2dFGRS ja SDSS, mis kokku katavad ära umbkaudu veerand taevast ning mis sisaldavad enam kui pool miljonit galaktikat.

Käesoleva töö peamiseks eesmärgiks on uurida, kuidas galaktikate evolutsioon sõltub Universumi suuremastaabilisest struktuurist ning kuivõrd erinevad on galaktikate evolutsiooni põhiprotsessid galaktikaparvede tsentraalsete, satelliitgalaktikate ja isoleeritud galaktikate jaoks. Uurimiseks kasutame praeguse hetke suurimaid galaktikate ülevaateid 2dFGRS ja SDSS. Universumi suuremastaabilise struktuuri kirjeldamiseks kasutame heledus-tiheduse välja, mis pärast vaatluslikke ja selektsiooni parandeid võimaldab küllalt usaldusväärselt eristada Universumis eri tihedusega piirkondi: tühikuid, filamente ja superparvi. Galaktika gruppide uurimiseks kasutame galaktika gruppide ja parvede kataloogi, mis võimaldab eristada grupi tsentraalseid ja satelliitgalaktikaid ning isoleeritud galaktikaid.

Galaktikate evolutsiooni jälgimiseks kasutame galaktikate heledusfunktsiooni, mis on üks fundamentaalsemaid meetodeid vaatluslikus kosmoloogias. Me võrdleme galaktikate heledusfunktsiooni taevaülevaadete erinevatel alamvalimitel ning teeme sellest järeldusi galaktikate evolutsiooni määravate protsesside kohta. Galaktikad jagame alamvalimiteks nende morfoloogia (spiraalsed, elliptilised) ning värvuse (punased, sinised) alusel. Samuti uurime heledusfunktsiooni eraldi galaktikagruppide tsentraalsete, satelliit ja isoleeritud galaktikate jaoks. Kõiki eelpool nimetatud valimeid vaatleme sõltuvana suuremastaabilisest struktuurist ehk globaalsest tihedusest.

Galaktikate heledusfunktsiooni arvutamine eeldab, et me teame galaktikate tegelikke heledusi. Vaadeldud galaktikate heledused sõltuvad paraku sellest, kas ja kui palju on galaktikates tolmu. Galaktikasisene tolm neelab galaktika tähtede valgust ning seega näeme vaadeldud galaktikat nõrgemana. Kuna tolmu on märkimisväärses koguses eelkõige spiraalgalaktikatel, siis spiraalgalaktikate vaadeldud heledus on neeldumisest kõige rohkem mõjutatud. Antud töös korrigeerime spiraalgalaktikate heledusi, et taastada galaktikate tegelik heledus. Neeldumise korrektuuri arvutamiseks kasutasime üksiku galaktika detailset modelleerimist. Selline ühe galaktika detailne modelleerimine võimaldas kindlaks teha, et neeldumine galaktikas sõltub nii galaktika sisemisest struktuurist kui ka kaldenurgast, mille all galaktika meile paistab. Galaktikates, kus domineerib mõhn, on neeldumine suurem kui galaktikates, kus domineerib ketas. Galaktika kaldenurgast sõltuvuse analüüs näitas, et neeldumine on suurim peaaegu serviti paistvate galaktikate korral. Arvutuste tulemusena selgus, et tolmu korrektsioon mõjutab spiraalgalaktikate heledusi kuni kaks korda.

Uurides galaktikate heledusfunksiooni grupi galaktikatele ning isoleeritud galaktikatele, järeldasime, et näivalt isoleeritud galaktikad ei pruugi olla täielikult isoleeritud. Enamus näivalt isoleerituid galaktikaid on pigem grupi tsentraalsed (heledaimad) galaktikad. Visuaalselt isoleeritud galaktikate olemasolu galaktikate valimis on tingitud suures osas vaatluslikust selektsioonist: galaktikate ülevaadetes vaadeldakse ainult teatud heledusest heledamaid galaktikaid. Sellise vaatlusliku selektsiooniga registreeritakse paljudes gruppides ainult heledaim galaktika ning grupi ülejäänud

galaktikad jäävad vaatlemata. Analüüs grupi heledamate ja heleduselt järgmiste galaktikate kohta näitas, et heledusfunktsioon grupi heledamatele galaktiatele alatihedusega piirkondades langeb kokku heledusfunktsiooniga grupi heleduselt teistele galaktikatele ületihedusega piirkondades. See tulemus viitab, et suure tihedusega piirkondades olevad grupi heleduselt teised galaktikad on oma varasemas arengus tõenäoliselt olnud grupi tsentraalsed (heledaimad) galaktikad, enne kui see grupp on ühinenud mõne suurema grupiga. Saadud tulemus on kooskõlas hierarhilise kuhjumise teooriaga.

Uurides galaktikate heledusfunktsiooni sõltuvana suuremastaabilisest struktuurist, järeldasime, et elliptiliste galaktikate evolutsioon sõltub tugevalt ümbritsevast suuremastaabilisest keskkonnast, seevastu spiraalsete galaktikate heledusfunktsioon jääb erineva tihedusega piirkondades muutumatuks. Elliptiliste galaktikate heleduste üldine sõltuvus globaalsest keskkonnast oli oodatav, kuna elliptilised galaktikad tekivad vastavalt praegusele galaktikate tekke paradigmale peamiselt galaktikate ühinemise tulemusel ning tihedamates piirkondades on galaktikate ühinemisi keskmiselt rohkem. Spiraalgalaktikate heledusfunktsiooni sarnasus erinevates piirkondades viitab, et spiraalgalaktikate tekkimine erinevates keskkondades on sarnane. Kuna hierarhilise kuhjumise teooria järgi peaks ka spiraalgalaktikatel olema sõltuvus ümbritsevast globaalsest keskkonnast, siis antud tulemus viitab, et spiraalgalaktikate tekkimiseks on vajalikud spetsiifilised tingimused. Antud tulemuse detailne analüüs nõuab põhjalikumaid uurimusi, mis on jäetud edaspidiseks.

Heledusfunktsiooni analüüs sõltuvana galaktikate morfoloogilisest tüübist osutas, et heledate galaktikate hulgas domineerivad elliptilised galaktikad ning nõrgemate galaktikate hulgas domineerivad spiraalsed galaktikad. Eelpool mainitud trend on ka globaalsest keskkonnast sõltuv: tihedamates piirkondades domineerivad heledamas otsas elliptilised galaktikad jõulisemalt kui hõredamas piirkonnas. Kui vaadelda ainult tühikuid suuremastaabilises struktuuris, siis seal domineerivad kogu heledusvahemikus spiraalgalaktikad. See viitab samuti asjaolule, et elliptilite galaktikate tekkimises on olulised galaktikte omavahelised põrked ja ühinemised, mida hõredates piirkondades esineb keskmisest vähem.

Antud töö keskendus galaktikate evolutsiooni vaatluslikule uurimisele ning töö tulemusi saab edaspidi rakendada vastavates numbrilistes ning pool-analüütilistes mudelites, mis võimaldavad täpsemalt määrata, millised füüsikalised protsessid on olulised erinevates keskkondades. Käesoleva töö tulemused näitasid selgelt, et lisaks lokaalsele (gruppide) keskkonnale on galaktikate evolutsioonis oluline ka globaalne, suuremastaabiline ümbrus. Loodetavasti aitab suuremastaabilise keskkonna mõju arvestamine lahendada mõnesid huvipakkuvaid probleeme galaktikate tekke stsenaariumites.

PUBLICATIONS

CURRICULUM VITAE

Personal data

Name	Elmo Tempel
Date and place of birth	16 June 1980, Paide, Estonia
Citizenship	Estonian
Marital status	married
Current employment	Tartu Observatory (research associate)
Address	Tartu Observatory 61602 Tõravere Tartumaa, Estonia
Phone	(+372) 50 79 048
E-mail	elmo@aai.ee

Education

1987 – 1999	Türi Economic Gymnasium
1999 – 2003	University of Tartu, undergraduate student, BSc 2003 (astrophysics)
2003 – 2005	University of Tartu, graduate student, MSc 2005 (astrophysics)
2005 – 2011	University of Tartu, PhD student

Employment

2005 – 2010	Tartu Observatory, extraordinary research associate
2010 – . . .	Tartu Observatory, research associate

Professional training

03.09 – 07.09 2007	Summer school "The Finnish graduate school in astronomy and space physics 2007: time series analysis", Elva, Estonia
10.09 – 21.09 2007	Summer school "Novicosmo 2007: fiat lux – formation and evolution of cosmic structures", Novigrad, Cittanova, Croatia
30.06 – 04.07 2008	Summer school "Cosmology: an astrophysical perspective", Heraklion, Crete, Greece
17.11 – 28.11 2008	Winter school "XX Canary Islands winter school of

	astrophysics: Local Group cosmology", Puerto de la Cruz, Tenerife, Spain
28.03 – 02.04 2009	Summer school "EuroVO-AIDA school 2009", Garching, Germany
18.05 – 20.05 2009	Summer school "Scientific writing for young astronomers", Blankenberge, Belgium
01.07 – 03.07 2009	Summer school "International summer school: future cosmic sky surveys and huge databases", Tartu, Estonia
12.06 – 20.06 2010	Summer school "CSC summer school in scientific and high-performance computing", Espoo, Finland

Conference presentations

16.07 – 20.07 2007	Conference "Galaxy growth in a dark Universe", Heidelberg, Germany. *Poster presentation*: "Dark matter distribution and a self-consistent model of the Andromeda galaxy"
03.10 – 05.10 2007	Conference "Tuorla and Tartu Observatories autumn meeting in cosmology and large-scale structure", Tuorla, Finland. *Oral presentation*: "Dark matter distribution and a self-consistent model of the Andromeda galaxy"
01.10 – 04.10 2008	Conference "Tartu – Tuorla annual meeting 2008. Cosmology: from observations to simulations and beyond", Tartu, Estonia. *Oral presentation*: "Anatomy of luminosity functions"

Language skills

Estonian	the first language
English	good
German	basic

Honours and Awards

2005	E. Öpik stipend (Tartu Observatory)
2008	E. Öpik stipend (Tartu Observatory)

Fields of research

Photometrical and dynamical modelling of galaxies.
Galaxy and group evolution in large-scale environment.

Publications

1. **Tempel, E.**, & Tenjes, P. 2006, *Line-of-sight velocity dispersions and a mass-distribution model of the Sa galaxy NGC 4594*, Monthly Notices of the Royal Astronomical Society, 371, 1269–1279.
2. Tamm, A., **Tempel, E.**, & Tenjes, P. 2007, *Visible and dark matter in M 31. I. Properties of stellar components*, arXiv:0707.4375v3 [astro-ph] (11 pages)
3. **Tempel, E.**, Tamm, A., & Tenjes, P. 2007, *Visible and dark matter in M 31. II. A dynamical model and dark matter density distribution*, arXiv:0707.4374v2 [astro-ph] (12 pages)
4. Tago, E., Einasto, J., Saar, E., **Tempel, E.**, Einasto, M., Vennik, J., & Müller, V. 2008, *Groups of galaxies in the SDSS Data Release 5. A group-finder and a catalogue*, Astronomy & Astrophysics, 479, 927–937
5. Nurmi, P., Heinämäki, P., Niemi, S., Saar, E., Tago, E., Einasto, M., **Tempel, E**., Einasto, J., & Martínez, V. J. 2008, *Galaxy groups in ΛCDM simulations and SDSS DR6*, Proceedings of the international conference held at Russian Geographical Society, Problems of practical cosmology, ed. by Y. V. Baryshev, I. N. Taganov, and P. Teerikorpi, Vol. 1, p78–85
6. Heinämäki, P., Nurmi, P., Tago, E., Saar, E., Liivamägi, L. J., **Tempel, E.**, Einasto, M., Einasto, J., Lietzen, H., & Takalo, L. 2008, *Nearby quasars in SDSS*, Proceedings of the international conference held at Russian Geographical Society, Problems of practical cosmology, ed. by Y. V. Baryshev, I. N. Taganov, and P. Teerikorpi, Vol. 1, p123–128
7. **Tempel, E.**, Einasto, J., Einasto, M., Saar, E., Tago, E. 2009, *Anatomy of luminosity functions: the 2dFGRS example*, Astronomy & Astrophysics, 495, 37–51
8. Tamm, A., **Tempel, E.**, & Tenjes, P. 2009, *Luminous and dark matter in the Andromeda galaxy*, Proceedings of the International Astronomical Union, IAU Symposium, Volume 254, The galaxy disk in cosmological context, ed. J. Andersen, J. Bland-Hawthorn, and B. Nordström, p73
9. Lietzen, H., Heinämäki, P., Nurmi, P., Tago, E., Saar, E., Liivamägi, J., **Tempel, E.**, Einasto, M., Einasto, J., Gramann, M., & Takalo, L. O. 2009, *Environments of nearby quasars in Sloan Digital Sky Survey*, Astronomy & Astrophysics, 501, 145–155
10. Martínez, V. J., Arnalte-Mur, P., Saar, E., de la Cruz, P., Pons-Bordería, M. J., Paredes, S., Fernández-Soto, A., & **Tempel, E**. 2009, *Reliability of the detection of the baryon acoustic peak*, Astrophysical Journal Letters, 696, L93–L97
11. **Tempel, E.**, Tamm, A., & Tenjes, P. 2010, *Dust-corrected surface photometry*

of M 31 from Spitzer far-infrared observations, Astronomy & Astrophysics, 509, A91 (13 pages)

12. Tago, E., Saar, E., **Tempel, E.**, Einasto, J., Einasto, M., Nurmi, P., & Heinämägi, P. 2010, *Groups of galaxies in the SDSS Data Release 7. Flux- and volume-limited samples*, Astronomy & Astrophysics, 514, A102 (11 pages)
13. Lietzen, H., Heinämäki, P., Nurmi, P., Liivamägi, L. J., Saar, E., Tago, E., **Tempel, E.**, Einasto, M., Einasto, J., Gramann, M., & Takalo, L. O. 2010, *Large Scale Environments of Nearby Quasars*, AIP Conference Proceedings, Hunting for the dark: the hidden side of galaxy formation, ed. V. P. Debattista and C. C. Popescu, Vol. 1240, p249–250
14. Einasto, M., Tago, E., Saar, E., Nurmi, P., Enkvist, I., Einasto, P., Heinämäki, P., Liivamägi, L. J., **Tempel, E.**, Einasto, J., Martínez, V. J., Vennik, J., & Pihajoki, P. 2010, *The Sloan great wall. Rich clusters*, Astronomy & Astrophysics, 522, A92 (19 pages)
15. **Tempel, E.**, Tuvikene, T., Tamm, A., & Tenjes, P. 2011, *SDSS surface photometry of M 31 with absorption corrections*, Astronomy & Astrophysics, 526, A155 (6 pages)
16. **Tempel, E.**, Saar, E., Liivamägi, L. J., Tamm, A., Einasto, J., Einasto, M., & Müller, V. 2011, *Galaxy morphology, luminosity, and environment in the SDSS DR7*, Astronomy & Astrophysics, 529, A53 (14 pages)
17. Liivamägi, L. J., **Tempel, E.**, & Saar, E. 2011, *SDSS DR7 superclusters. The catalogues*, Astronomy & Astrophysics, submitted, arXiv:1012.1989
18. Suhhonenko, I., Einasto, J., Liivamägi, L. J., Saar, E., Einasto, M., Hütsi, G., Müller, V., Starobinsky, A. A., Tago, E., & **Tempel, E.** 2011, *The cosmic web for density perturbations of various scales*, Astronomy & Astrophysics, accepted for publication, arXiv:1101.0123
19. Einasto, J., Hütsi, G., Saar, E., Suhhonenko, I., Liivamägi, L. J., Einasto, M., Müller, V., Tago, E., Starobinsky A. A., & **Tempel, E.** 2011, *Wavelet analysis of the formation of the cosmic web*, Astronomy & Astrophysics, submitted, arXiv:1012.3550
20. Tamm, A., **Tempel, E.**, & Tenjes, P. 2011, *Luminous and dark matter in the Andromeda galaxy*, Proceedings of the International Astronomical Union, IAU Symposium, Volume 277, Tracing the ancestry of galaxies
21. Einasto, M., Liivamägi, L. J., Tago, E., Saar, E., **Tempel, E.**, Einasto, J., Martínez, V. J., & Heinämäki, P. 2011, *SDSS superclusters. Morphology*, Astronomy & Astrophysics, submitted

ELULOOKIRJELDUS

Isikuandmed

Nimi	Elmo Tempel
Sünniaeg ja -koht	16. juuni 1980, Paide, Eesti
Kodakondsus	eesti
Perekonnaseis	abielus
Praegune töökoht	Tartu Observatoorium (teadur)
Aadress	Tartu Observatoorium 61602 Tõravere Tartumaa, Eesti
Telefon	(+372) 50 79 048
E-post	elmo@aai.ee

Haridustee

1987 – 1999	Türi Majandusgümnaasium
1999 – 2003	Tartu Ülikool, üliõpilane, BSc 2003 (astrofüüsika)
2003 – 2005	Tartu Ülikool, magistrant, MSc 2005 (astrofüüsika)
2005 – 2011	Tartu Ülikool, doktorant

Teenistuskäik

2005 – 2010	Tartu Observatoorium, erakorraline teadur
2010 – . . .	Tartu Observatoorium, teadur

Täiendkoolitus

03.09 – 07.09 2007	Suvekool “The Finnish graduate school in astronomy and space physics 2007: time series analysis”, Elva, Eesti
10.09 – 21.09 2007	Suvekool “Novicosmo 2007: fiat lux – formation and evolution of cosmic structures”, Novigrad, Horvaatia
30.06 – 04.07 2008	Suvekool “Cosmology: an astrophysical perspective”, Heraklion, Kreeta, Kreeka
17.11 – 28.11 2008	Talvekool “XX Canary Islands winter school of astrophysics: Local Group cosmology”, Puerto de la Cruz, Tenerife, Hispaania
28.03 – 02.04 2009	Suvekool “EuroVO-AIDA school 2009”, Garching, Saksamaa

18.05 – 20.05 2009	Suvekool “Scientific writing for young astronomers”, Blankenberge, Belgia
01.07 – 03.07 2009	Suvekool “International summer school: future cosmic sky surveys and huge databases”, Tartu, Eesti
12.06 – 20.06 2010	Suvekool “CSC summer school in scientific and high-performance computing”, Espo, Soome

Konverentside ettekanded

16.07 – 20.07 2007	Konverents “Galaxy growth in a dark Universe”, Heidelberg, Saksamaa. *Posterettekanne*: “Dark matter distribution and a self-consistent model of the Andromeda galaxy”
03.10 – 05.10 2007	Konverents “Tuorla and Tartu Observatories autumn meeting in cosmology and large-scale structure”, Tuorla, Soome. *Suuline ettekanne*: “Dark matter distribution and a self-consistent model of the Andromeda galaxy”
01.10 – 04.10 2008	Konverents “Tartu – Tuorla annual meeting 2008. Cosmology: from observations to simulations and beyond”, Tartu, Eesti. *Suuline ettekanne*: “Anatomy of luminosity functions”

Keelteoskus

eesti keel	emakeel
inglise keel	hea
saksa keel	vähene

Uurimistoetused ja stipendiumid

2005	E. Öpik stipendium (Tartu Observatoorium)
2008	E. Öpik stipendium (Tartu Observatoorium)

Peamised uurimissuunad

Galaktikate fotomeetriline ja dünaamiline modelleerimine.
Galaktikate ja galaktikaparvede evolutsioon Universumis.